NUREG/CR-1361
EGG-2025

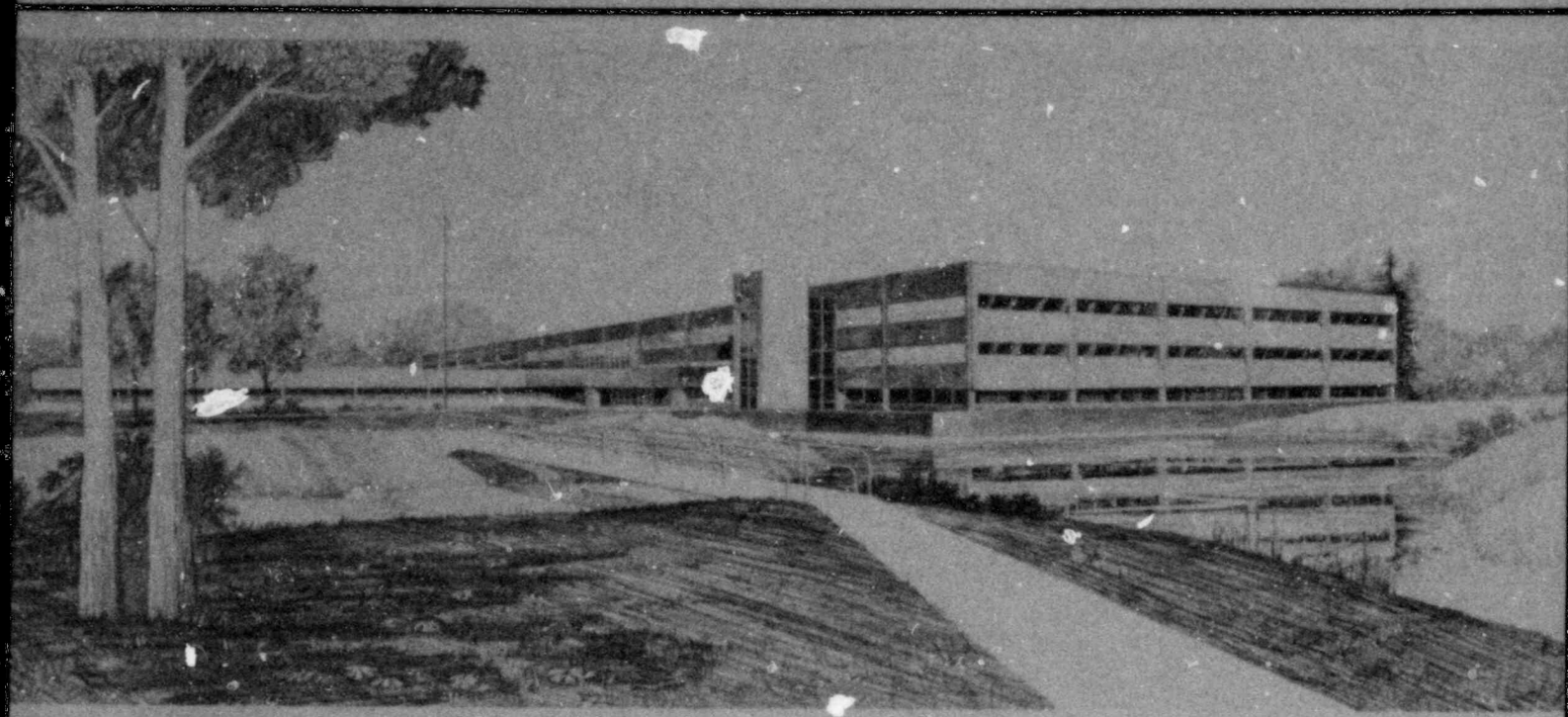

U.S. Department of Energy
Idaho Operations Office • Idaho National Engineering Laboratory

Drag Devices For Two-Phase Mass Flow Measurements

James L. Anderson

May 1980

Prepared for the
U. S. Nuclear Regulatory Commission
Washington, D. C. 20555
Under DOE Contract No. DE-AC07-76IDO1570

EG&G Idaho

Available fr[illegible]

GPO Sales Program
Division of Technical Information and Document Control
U.S. Nuclear Regulatory Commission
Washington, D.C. 20555

and

National Technical Information Service
Springfield, Virginia 22161

NUREG/CR-1361
EGG-2025
Distribution Category: R2

DRAG DEVICES FOR TWO-PHASE MASS FLOW MEASUREMENTS

James L. Anderson

Published May 1980

EG&G Idaho, Inc.
Idaho Falls, Idaho 83415

Prepared for the
U. S. Nuclear Regulatory Commission
Washington, D. C. 20555
Under DOE Contract No. DE-AC07-76IDO1570
FIN No. A6038

ABSTRACT

Results are presented from testing a number of full-flow drag devices in steady-state air-water mixtures and transient steam-water mixtures for the purpose of obtaining two-phase mass flow measurements. Modeling methods for obtaining mass flow rates are discussed along with the effects of two-phase flows on the drag coefficient of full-flow, multihole drag plates. Test results indicate that for applications in small piping, a multihole drag plate with a flow blockage of 23% provided the greatest accuracy of the devices tested, resulting in a normalized standard deviation of 2.5% for two-component mixtures. For low density, high velocity flows (such as all gas and annular mist flows) the drag coefficient of the drag device increased from its constant all water value, reflecting the effects of compressibility. For annular mist flows, the increase in the drag coefficient can be correlated to a parameter equal to the void fraction times the mass velocity of the mixture. Results are presented for eight different drag devices tested in air-water mixtures. Transient steam-water tests were performed to assess the transient performance of a prototype drag plate and to determine with what accuracy the mass exiting the system could be measured. Results from four partial blowdown tests are presented. Maximum error of these four blowdowns in measuring the total expelled mass was 10.4%.

NRC FIN NO. A6038
Semiscale Program

ACKNOWLEDGMENTS

James R. Fincke performed the design work of the original multihole drag plates, in addition to being responsible for all of the testing and results for the LOFT prototype drag plate. James B. Colson designed the drag screen prototype and was responsible for some of the first air-water testing of drag devices at the INEL. Rex W. Shumway assisted in using the Hughmark-Pressburg slip correlation, and Thomas K. Larson assisted in development of a two-phase drag coefficient correlation. Edgar M. Feldman and M. Douglas McKenzie performed the actual air-water tests.

SUMMARY

The Semiscale and Loss-of-Fluid-Test (LOFT) projects, located at the Idaho National Engineering Laboratory, are scaled integral test facilities that provide thermal-hydraulic information during postulated loss-of-coolant experiments to be used for nuclear safety studies involving pressurized water reactors. One of the basic quantities of interest during a loss-of-coolant experiment is the transient two-phase mass flow rate at various locations throughout the experimental system. One of the most reliable methods currently available for obtaining this quantity is to measure the momentum flux of the fluid, using a full-flow drag device, and to combine that measurement with a density measurement from a densitometer system. The equations are given that are used to obtain the two-phase mass flow rate from the combination of drag device and densitometer measurements; methods are also presented for obtaining momentum flux of the fluid from the drag device and the cross-sectional average density from the densitometer system. A comprehensive testing program in steady-state air-water mixtures has been performed to investigate the performance of various full-flow drag devices and to assess the accuracy of the measurement technique. For applications in small piping, a multihole drag plate with a flow blockage of 23% provided the greatest accuracy of those devices tested, resulting in a normalized standard deviation of 2.5% for two-component mixtures. For low-density, high-velocity flows (such as all gas and annular mist flows), the drag coefficient of the drag device increased from its constant all water value, reflecting the effects of compressibility.

For annular mist flows, this increase in the drag coefficient could be correlated to a parameter equal to the void fraction times the mass velocity of the mixture. Results are presented for eight different drag devices tested in air-water mixtures.

Several transient steam-water tests were performed in the LOFT Test Support Facility Blowdown Loop to assess the transient performance of the LOFT prototype drag plate and to determine with what accuracy the mass exiting the system could be measured. Results from four partial blowdowns are presented. The maximum error of these four blowdowns in measuring the total expelled mass was 10.4%.

Semiscale is currently the primary user and tester of full-flow drag devices for two-phase, mass flow rate measurements, with nine different measurement locations in the Semiscale Mod-3 system. The drag devices at these locations are briefly described in the report. Results are provided for two measurement locations during a Semiscale test. Intended future applications of full-flow drag devices in the LOFT system are discussed; the primary intended application is for measurement of the break mass flow rate during a loss-of-coolant experiment that simulates a small break in the primary coolant system (such as the type that occurred in the Three Mile Island accident).

CONTENTS

FIGURES

TABLES

DRAG DEVICES FOR TWO-PHASE MASS FLOW MEASUREMENTS

1. INTRODUCTION

The U. S. Nuclear Regulatory Commission (NRC) has the responsibility for licensing and insuring the safety of nuclear power plants within the U. S. To fulfiil this responsibility the NRC has initiated numerous reactor safety studies, which involve several programs at the Idaho National Engineering Laboratory (INEL). Two of these programs are the Semiscale and Loss-of-Fluid Test (LOFT) programs, both of which use scaled integral test facilites.

The Semiscale Program is a continuing series of thermal-hydraulic experiments to generate data that can be applied to the development and assessment of analytical models for describing transient phenomena in water-cooled nuclear power plants. Emphasis is placed on acquiring integral system effects data that characterize the most significant thermal-hydraulic phenomena likely to occur in the primary coolant system of a nuclear plant during the depressurization (blowdown) and emergency core cooling (ECC) phases of a loss-of-coolant accident (LOCA). The experiments are performed with a test system that simulates the principal features of a nuclear plant but which is smaller in volume [approximately 1/1700 the volume of a pressurized water reactor (PWR)]. Nuclear heating is simulated in the experiments by a core composed of an array of electrically heated rods each of which has dimensional and heat flux characteristics similar to those of a nuclear fuel rod.

LOFT provides test data to assess and improve analytical methods used to predict PWR behavior under LOCA conditions, to evaluate the performance of PWR engineered safety features, particularly the emergency core cooling system (ECCS), and to assess the safety margins inherent in the performance of the engineered safety features.

The LOFT test facility was designed to simulate the major components and system responses of a PWR involved in a LOCA. The facility includes a containment structure, support buildings, and a test assembly that holds the 55-MW(t) pressurized water reactor. The reactor core, about 1.7 m long by 0.6 m diameter, contains 1,300 fuel rods of 4.00 wt percent U^{235}. The test assembly is a scaled facility approximately 1/60 the size of a modern PWR.

One of the basic quantities of interest during a loss-of-coolant experiment (LOCE) is the transient two-phase (steam-water) mass flow rate. One of the most reliable methods currently available for obtaining this quantity is to measure the momentum flux (ρv^2) of the fluid, using a full-flow drag device, and to combine that measurement with a density measurement from a densitometer system. Numerous drag device configurations have been developed and tested at the INEL.[1,2,3,4] A variety of densitometer systems have been developed at INEL. Results are summarized in this report from testing various types of full-flow drag devices used to obtain the cross-sectionally averaged momentum flux of the fluid. The objective for the use of a full-flow drag device is to obtain a total momentum flux measurement independent of momentum flux profiles.

The second section of this report covers the basic equations used for obtaining mass flow rates, momentum fluxes, and cross-sectional average densities. Single and two-phase effects on drag coefficients are also covered in this section. Results from air-water testing of numerous full-flow drag devices are provided in the third section. Air-water testing was performed to investigate the performance of various drag device configurations under the influence of two-component flows. The fourth section is a summary of results from several transient steam-water tests, conducted to assess the performance of a full-flow drag device under saturated fluid conditions and to determine with what accuracy the mass exiting a system could be measured. Applications of various drag devices within the Semiscale Mod-3 system are discussed in the fifth section. Future applications for full-flow drag devices within the LOFT system are discussed in the sixth section. The seventh section provides those conclusions reached from testing of full-flow drag devices.

2. BASIC EQUATIONS

The following sections present the basic equations used to obtain the two-phase mass flow rate from a combination of drag device and densitometer measurements. Also presented are the methods for obtaining the momentum flux of the fluid from the drag device and the cross-sectional average density from the densitometer system. All models are based on the two-velocity concept of two-phase flow in piping.

2.1 Mass Flow Rate

The basic method that is used for calculating the two-phase mass flow rate combines the fluid density and momentum flux in the following manner:

$$\dot{m} = \left[\bar{\rho}\ \overline{\rho v^2}\right]^{1/2} A = G\,A \qquad (1)$$

where

$\dot{m}$ = the total mass flow rate (kg/s)

$\bar{\rho}$ = the cross-sectional averaged density from the densitometer system (kg/m^3)

$\overline{\rho v^2}$ = the cross-sectional averaged momentum flux from the drag device ($kg/m \cdot s^2$)

A = the flow area (m^2)

G = the mass velocity ($kg/m^2 \cdot s$).

At first, this method appears to be applicable only to a homogeneous fluid (that is, the phasic velocity of the gas equals that of the liquid). However, the effects of slip between the phases is included in the density term and is discussed in more detail later.

2.2 Momentum Flux and Drag Coefficient

The momentum flux is obtained through use of a drag device by inserting a drag body of some type into the fluid flow and measuring the force exerted on the drag body by the fluid. This force is related to the momentum flux of the fluid through the relationship

$$F_D = \frac{1}{2}\left(C_D A_S \rho v^2\right) \qquad (2)$$

where

F_D = the measured drag force ($kg \cdot m/s^2 = N$)

C_D = the drag coefficient (nondimensional)

A_S = the frontal (or projected) area of the drag body (m^2)

ρv^2 = the average momentum flux across the drag body ($kg/m \cdot s^2$).

If the drag body being used is a full-flow type (that is, if the drag body is sampling the momentum flux of the fluid over the entire flow area), then the momentum flux in Equation (2) is the cross-sectionally average momentum flux for use in Equation (1). Figure 1 is a sketch of a typical full-flow drag device (in this case a hinged, multihole drag plate) indicating the forces exerted on the drag device.

Equation (2) reveals that the crucial parameter in obtaining the momentum flux from the measured drag force is the correct value for the drag coefficient. This quantity is typically obtained in fluid mechanics from experiment and is a function of the Reynolds Number. Fortunately, in the work described herein, the drag coefficient for certain geometries is a constant over a wide range of Reynolds Numbers. Figure 2 presents single-phase drag coefficients for a cylinder, disc, and multiholed plate (such as shown in Figure 1) versus Reynolds Number. For the disc and the multihole plate, the drag coefficient is constant over the Reynolds Number range of 10^4 to 10^7. Most flows of interest for water reactor safety research (and most other engineering applications) are in this range. The drag coefficient for the cylinder has a sudden and dramatic decrease in value at a Reynolds Number of about 200 000. This effect is traditionally explained as being due to a flow separation from the body.

The information presented in Figure 2 is typically presented in basic texts on fluid mechanics and is obtained from experiment using a number of different fluids, including air at the

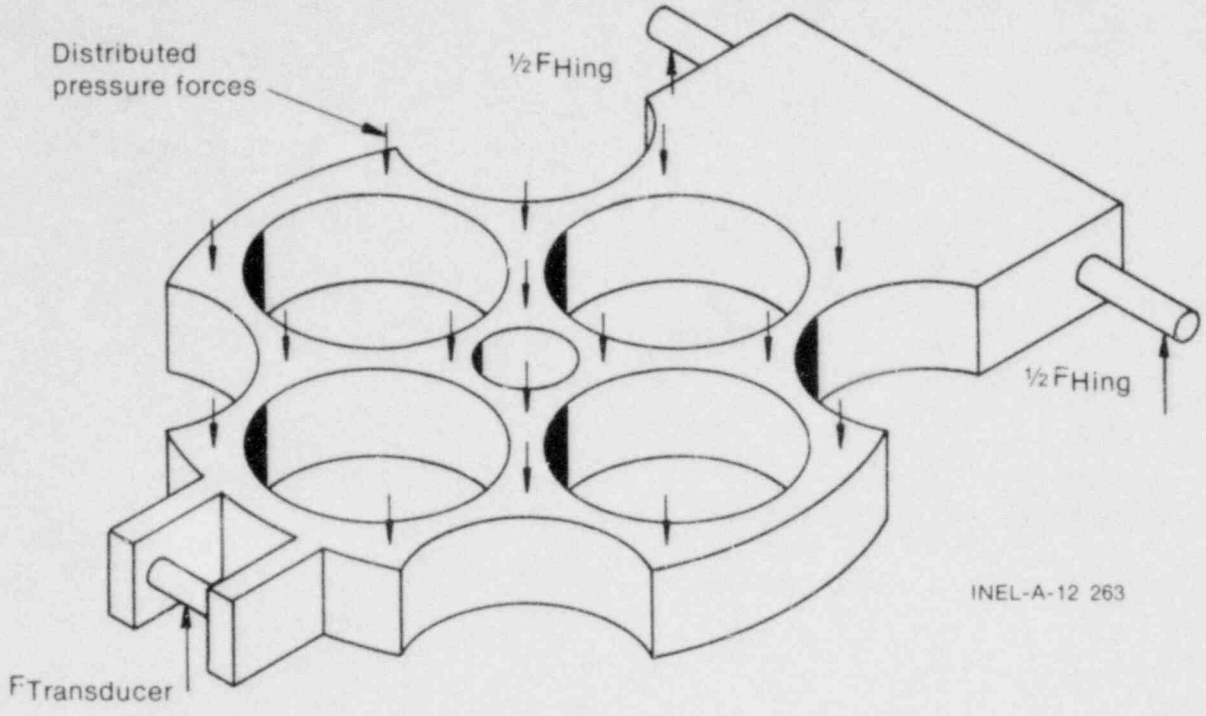

Figure 1. Hinged, multihole drag plate showing forces involved.

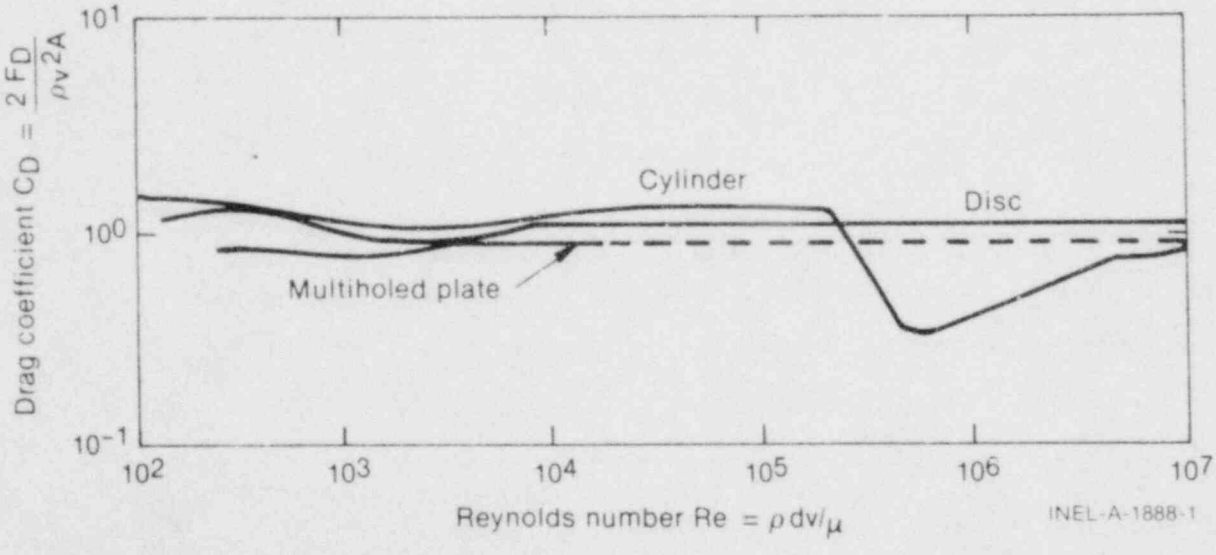

Figure 2. Single-phase drag coefficients for a cylinder, disc, and multihole plate.

lower Reynolds Numbers. The information presented in Figure 3 was compiled from extensive single-phase (water) calibration tests performed at the INEL on multihole drag plates. This figure shows that the single-phase drag coefficient for the multihole plate is not Reynolds Number dependent over the range in which it was tested. Figure 4 presents the drag coefficient for single-phase, all-air flows, versus the Mach number of the flow for the same drag plate. This information demonstrates the effect of compressiblity on the drag coefficient, with the result that the drag coefficient increases with increasing Mach number and appears to be increasing in a exponential manner as the Mach number approaches 1.0. For the lower flow rates (M <0.2), the drag coefficient can be treated as a constant, which is equal to the drag coefficient for water.

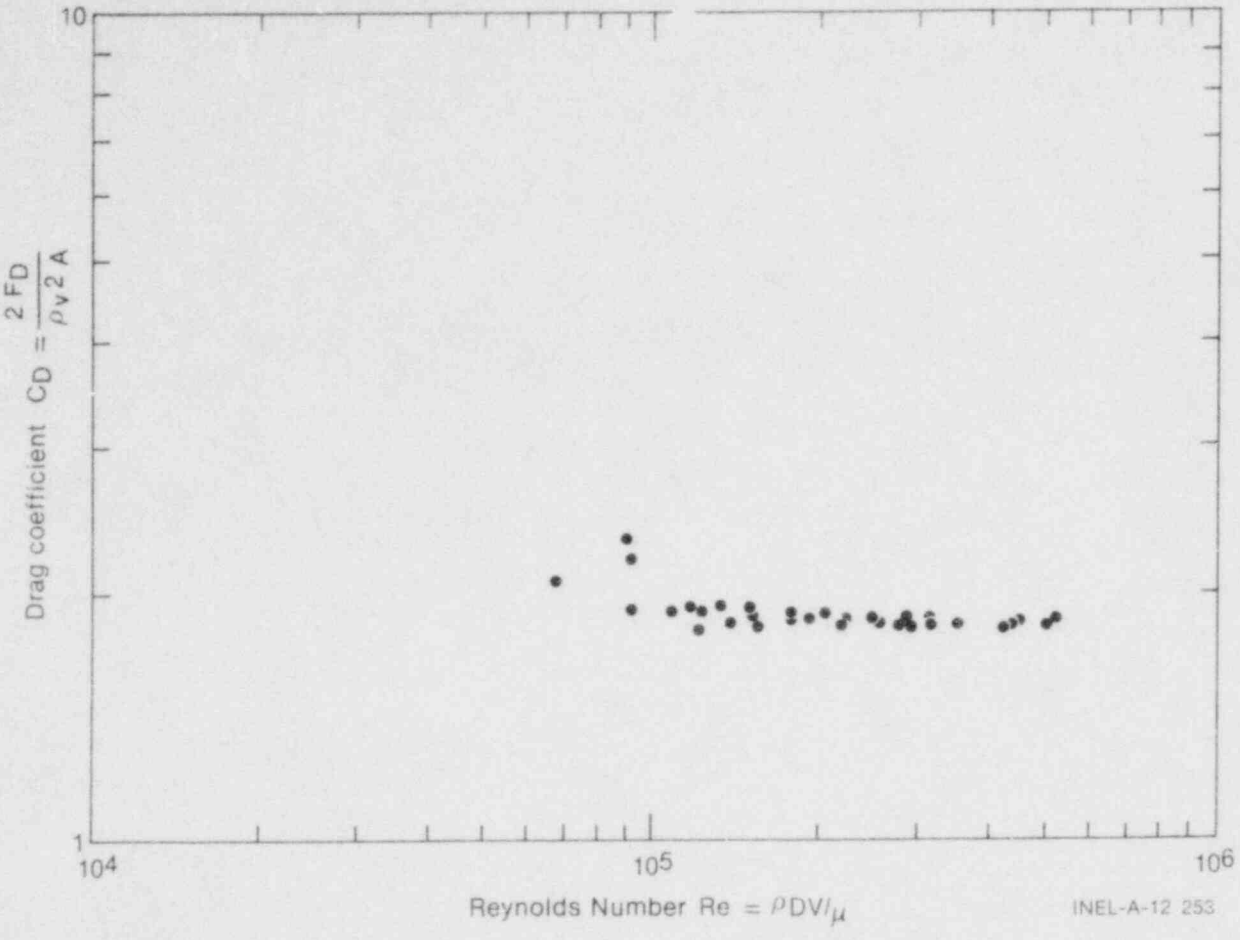

Figure 3. Single-phase (all-water) drag coefficient for multihole plate (3.40 cm ID piping) versus Reynolds Number.

The drag coefficients presented in Figures 3 and 4 were obtained by establishing a known, steady-state flow rate through a test section containing a hinged, multihole drag plate and measuring the drag force on the drag plate.[a] The momentum flux was calculated from the known flow rate and the fluid density at the test section. The drag coefficient was then calculated using the following relationship obtained from rearranging Equation (2)

$$C_D = \frac{2 F_D}{A_S \rho v^2} \tag{3}$$

a. For the hinged drag device, the total drag force F_D is equal to the force measured at the force transducer F_T times a constant due to the geometry of the drag plate. In this method, the summation of the distributed drag force is assumed to be centered on the portion of the drag plate exposed to the fluid flow. This assumption is valid as long as no upstream disturbance exists (such as an elbow) to create a skewed momentum flux profile, causing the centroid of the force to move away from the plate center in a horizontal plane.

where

$$\rho v^2 = \frac{\dot{m}_{sp}^2}{\rho_{sp} A^2} \tag{4}$$

and where

$\dot{m}_{sp}$ = the single-phase mass flow rate

ρ_{sp} = the single-phase density.

Determination of the two-phase effects on the drag coefficient is a much more difficult problem since the determination of the correct value of the momentum flux to be used in Equations (3) and (4) is not easily obtained. The known parameters are the individual mass flow rates and phasic densities at the test section. One other known parameter is the time-averaged and cross-sectionally averaged void fraction of the two-phase mixture, obtained from the densitometer system.

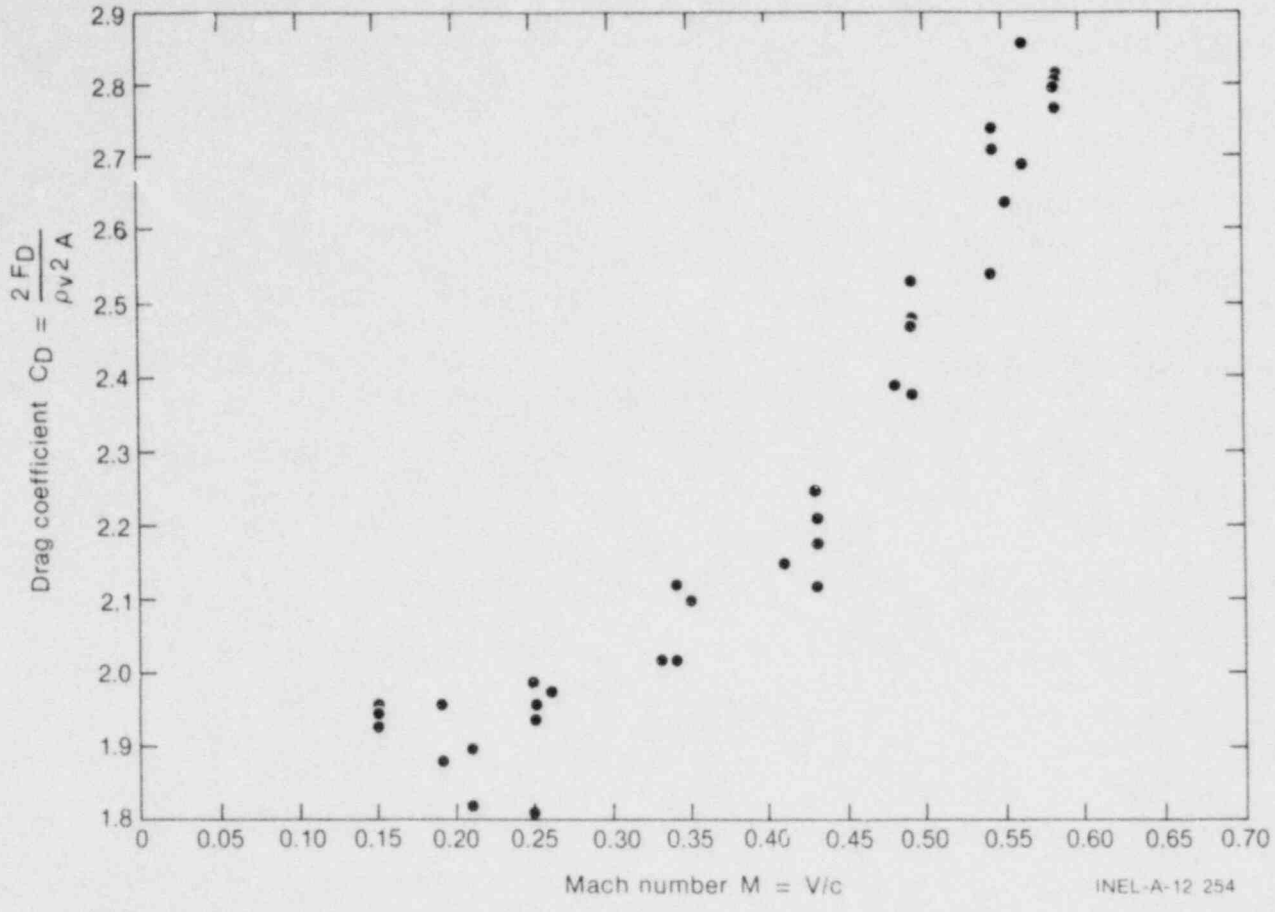

Figure 4. Single-phase (all-air) drag coefficient for drag plate (3.40 cm ID piping) versus Mach number.

The distribution of the two phases over the flow area may or may not be known, depending on the type of densitometer system used. Of importance is the fact that the cross-sectionally averaged, two-phase momentum flux is dependent on both the density and velocity distributions over the flow area. Thus, an accurate knowledge of both of these distributions is required to calculate the actual momentum flux at the test section. However, since this analysis is only concerned with cross-sectionally averaged properties, attempts to use the phase distributions across the flow area are not considered. Instead a two-velocity separated flow model, in which each phase is assumed to move at its own uniform and constant velocity is used.

The two-velocity momentum flux model is based on the assumption that the total drag force on the drag body is equal to the summation of the individual forces due to the gas and liquid phases, which are individually proportional to a drag coefficient times the momentum flux of that phase. The total drag force F_D is then

$$F_D = \left(\frac{1}{2}\right) C_D A_S \left[\alpha \rho_G V_G^2 + (1 - \alpha) \rho_F V_F^2\right] \quad (5)$$

where

C_D = single-phase drag coefficient

A_S = frontal area of the drag body

α = cross-sectional average void fraction of the mixture

V_G = gas phase velocity

V_F = liquid phase velocity

ρ_G and ρ_F = densities of the gas and liquid phases.

As was previously stated, this equation is based on a two-velocity model, in which all of the gas phase is flowing at V_G and all of the liquid phase is moving at V_F, and the equation is a direct result of integrating the flow over the flow area.

Since the mass flow rates of the individual phases can be represented by

$$\dot{m}_G = \alpha \rho_G V_G A \tag{6}$$

for the gas and

$$\dot{m}_F = (1-\alpha) \rho_F V_F A \tag{7}$$

for the liquid, the drag force can be represented by

$$F_D = \frac{A_S C_D}{2 A^2} \left[\frac{\dot{m}_G^2}{\alpha \rho_G} + \frac{\dot{m}_F^2}{(1-\alpha)\rho_F} \right] \tag{8}$$

where

$\dot{m}_G$ and $\dot{m}_F$ = the mass flow rates of gas and liquid phase, respectively.

Equating Equations (2) and (8), and solving for the momentum flux, results in the two-velocity model for the two-phase momentum flux, ρV^2,

$$\overline{\rho V^2} = \frac{1}{A^2} \left[\frac{\dot{m}_G^2}{\alpha \rho_G} + \frac{\dot{m}_F^2}{(1-\alpha)\rho_F} \right]. \tag{9}$$

Through use of the preceding definition for the two-phase momentum flux and the measured drag force on the hinged, multihole drag plate, the two-phase, air-water drag coefficients were calculated. These drag coefficients were calculated using the void fraction as measured by the scanning x-ray densitometer[a] and cover a void fraction range of 0.85 to 0.999. It was found that the two-phase drag coefficient could be correlated to a parameter, which is the void fraction times the mass velocity (αG). The two-phase drag coefficients versus this correlation parameter are presented in Figure 5. The drag coefficient

a. The basics of the scanning x-ray densitometer are described in next section, Density.

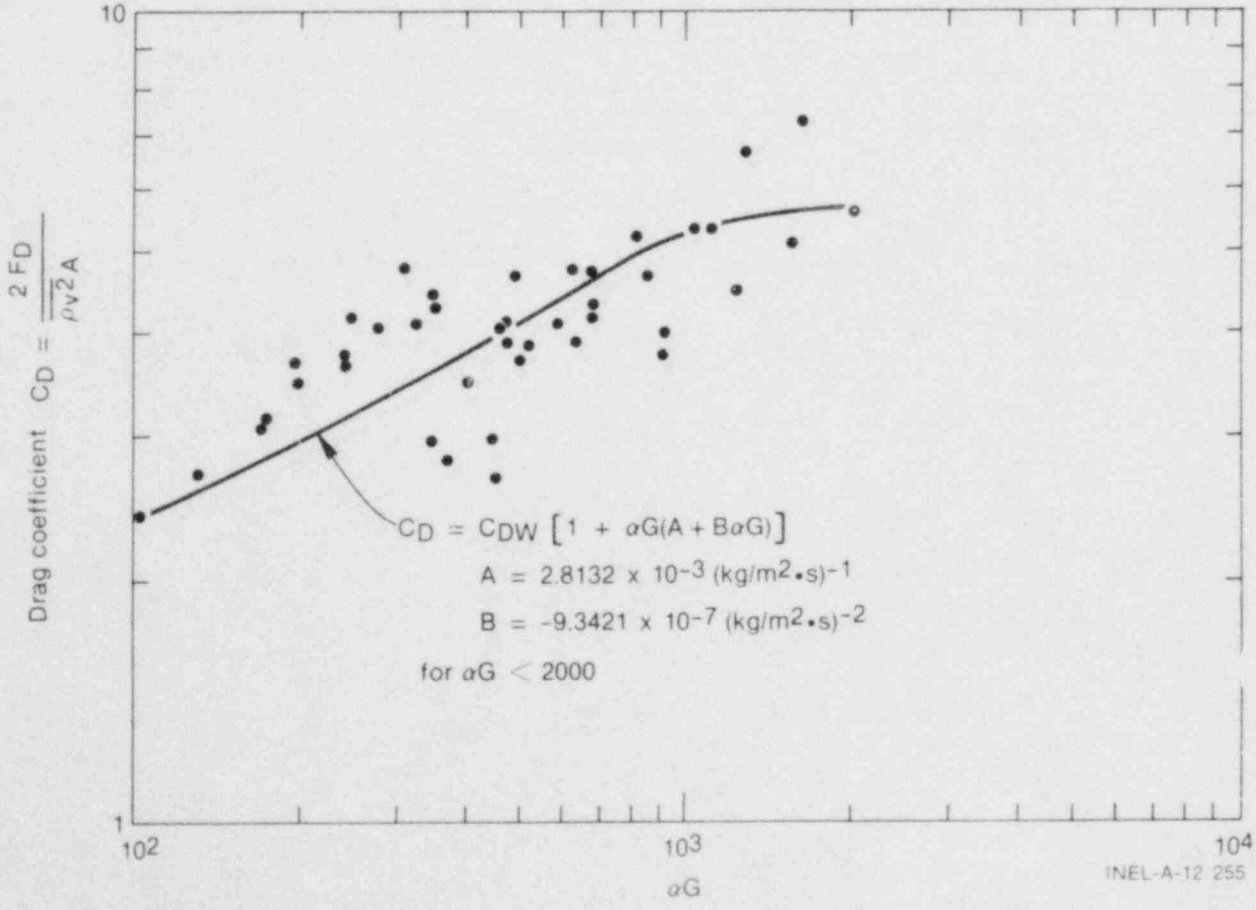

Figure 5. Two-phase drag coefficient for hinged, multihole drag plate (3.40 cm ID piping) versus αG for annular mist flows.

increases from its single-phase water value as the parameter αG increases ($\alpha G = 0$ is the all water case), eventually increasing by a factor of four over the single-phase value. To measure mass flow during two-phase fluid conditions using a full-flow drag device, this variation must be taken into account. The dependence of the drag coefficient on the αG parameter is not fully understood. However, the increase in the drag coefficient is postulated to be primarily due to compressibility effects and the αG parameter is postulated to be a function of the velocity of the fluid and the changing sonic velocity of the fluid (that is, the two-phase Mach number). The data presented in Figure 5 were fit with a quadratic equation resulting in

$$C_D = C_{DW} [1 + \alpha G (A + B\alpha G)]$$

where

C_{DW} = the single-phase (water) drag coefficient

A = the first order fit coefficient = 2.8132×10^{-3} $(kg/m^2 \cdot s)^{-1}$

B = the second order fit coefficient = -9.341×10^{-7} $(kg/m^2 \cdot s)^2$

The correlation was obtained for annular mist flows with void fractions ranging from 0.85 to 0.999 and is valid only for these types of flows in which the parameter αG is less than 2000 $kg/m^2 \cdot s$.

2.3 Density

Two different densitometer systems were used in the air-water testing being reported. For testing in 6.67 cm ID piping, a two-beam gamma densitometer was used. Figure 6 shows the beam orientation of the two-beam densitometer that was used. This densitometer system was designed for use on horizontal piping. A number of analytical models were examined for use in obtaining the cross-sectionally averaged density from this densitometer. The model that has proven to be the

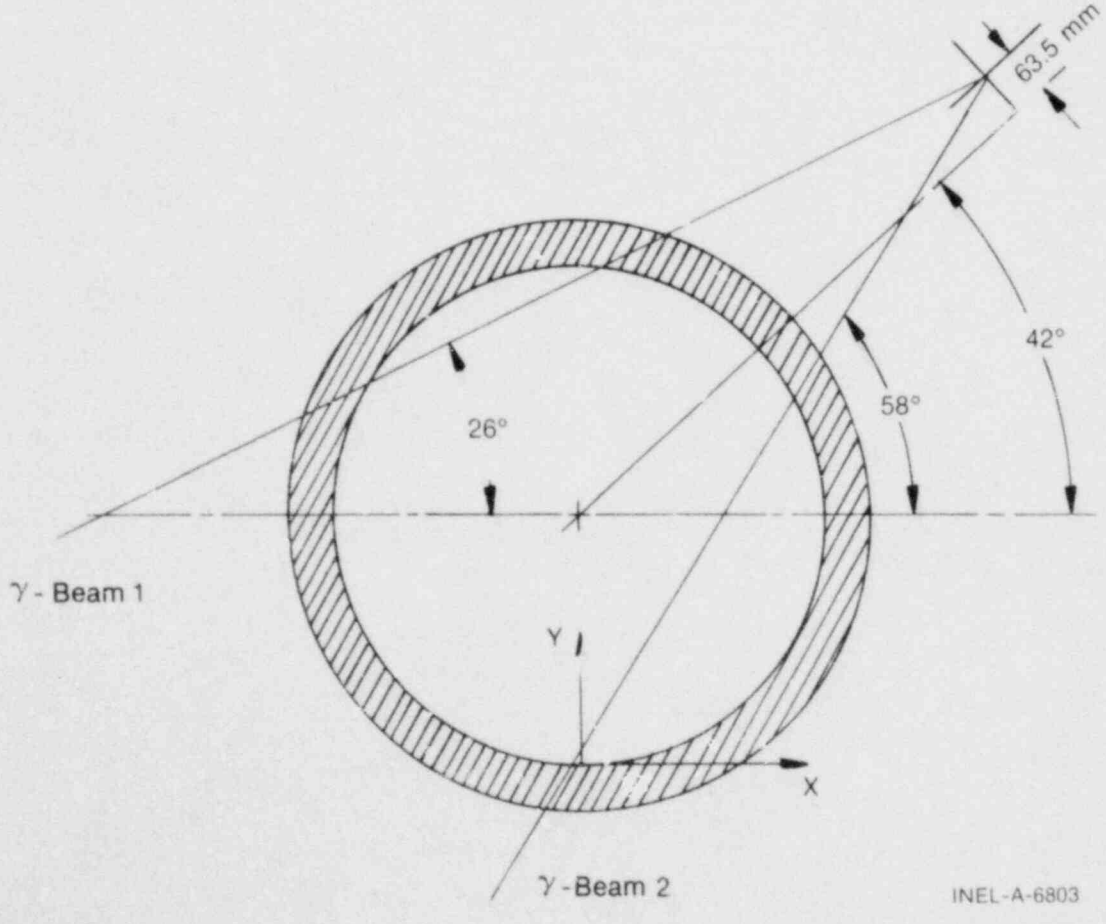

Figure 6. Beam geometry of two-beam gamma densitometer for 6.67 cm ID piping.

most accurate and independent of the flow regime is the continuous stratified model.[5] In this model, the density is assumed to vary only in the vertical direction in a continuous manner according to the following relationship

$$\rho(Y) = \rho_F - \frac{\rho_F - \rho_G}{1 + e^{-4a(Y-b)}} \qquad (10)$$

where

$\rho(Y)$ = the local density at elevation Y (kg/m^3)

Y = the vertical coordinate measured from the bottom of the pipe (m)

a and b = coefficients chosen to fit the data from the individual beams.

The coefficients a and b are chosen by a least-square fitting routine for a best fit to the data from the two-beam densitometer. Figure 7 shows the distributions for four flow regimes (dispersed bubble, bubbly slug, wavy stratified, and stratified mist) from data obtained in an air-water mixture using the two-beam gamma densitometer. This model provides realistic density distributions for all flow regimes observed in air-water testing, except annular mist. In addition, this model provides fairly accurate cross-sectional average densities ($\bar{\rho}$) for all flow regimes, including annular

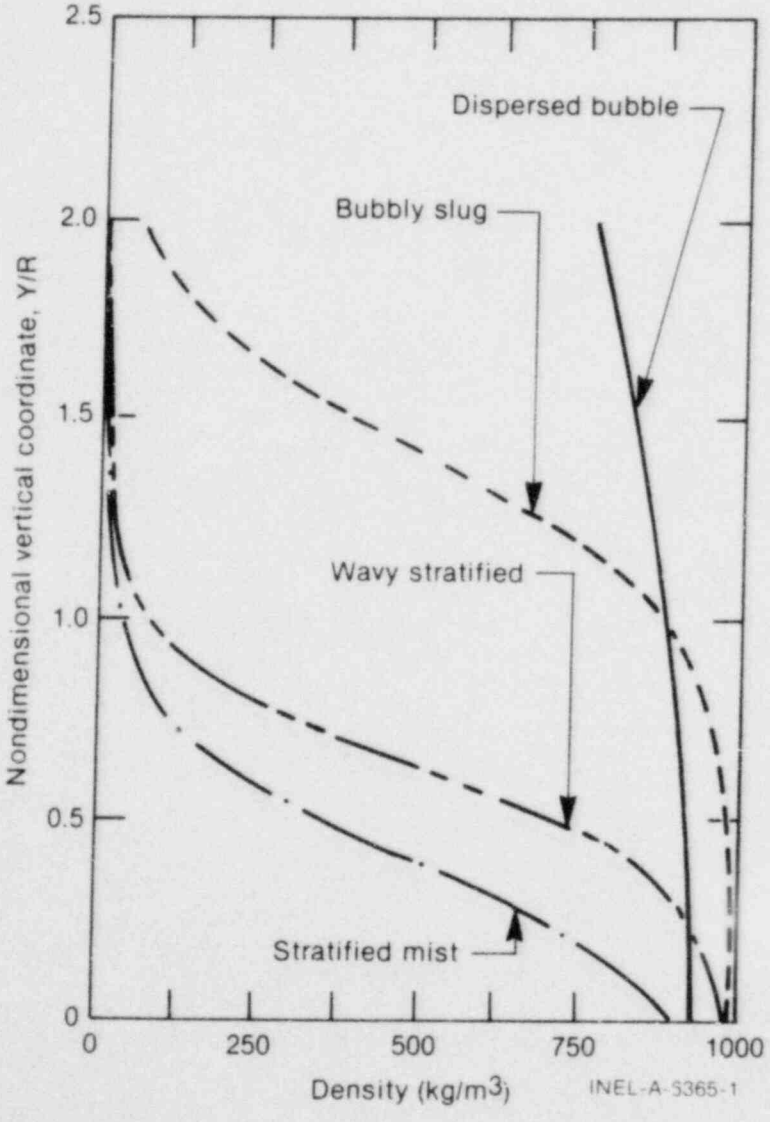

Figure 7. Typical density distributions obtained from the continuous stratified densitometer model [Equation (10)].

mist. The cross-section average density is obtained from Equation (10) by integrating over the pipe flow area.

The most accurate of the densitometer systems that has been developed to date is the scanning x-ray densitometer.[6] This densitometer system has proven to be extremely valuable in providing both density distribution information and accurate cross-sectional average densities. In addition, this densitometer system has been used to verify the accuracy of the cross-sectional average density as obtained from the continuous stratified densitometer model. In this densitometer system, the source used is a characteristic x-ray emitter[a] fixed on one side of the pipe. A detector on the other side of the pipe scans across the pipe diameter. A sketch of the basic configuration is provided in Figure 8.

The average density obtained from the densitometer system (either the two-beam gamma densitometer system or the scanning x-ray densitometer) is used to calculate the cross-sectional average void fraction as follows

$$\alpha = \frac{\rho_F - \bar{\rho}}{\rho_F - \rho_G} \tag{11}$$

In the two-velocity model of the two-phase fluid flow, the average density used to calculate the two-phase mass flow rate includes the effect of the ratio of the individual phase velocities. This ratio is termed the slip ratio and is defined by

$$S = \frac{V_G}{V_F} \tag{12}$$

where

S = the slip ratio

V_G and V_F = the actual average phase velocities of the gas and fluid phases at the test section.

a. A Cd-109 source with 22- and 27-keV characteristic x-rays has been used extensively.

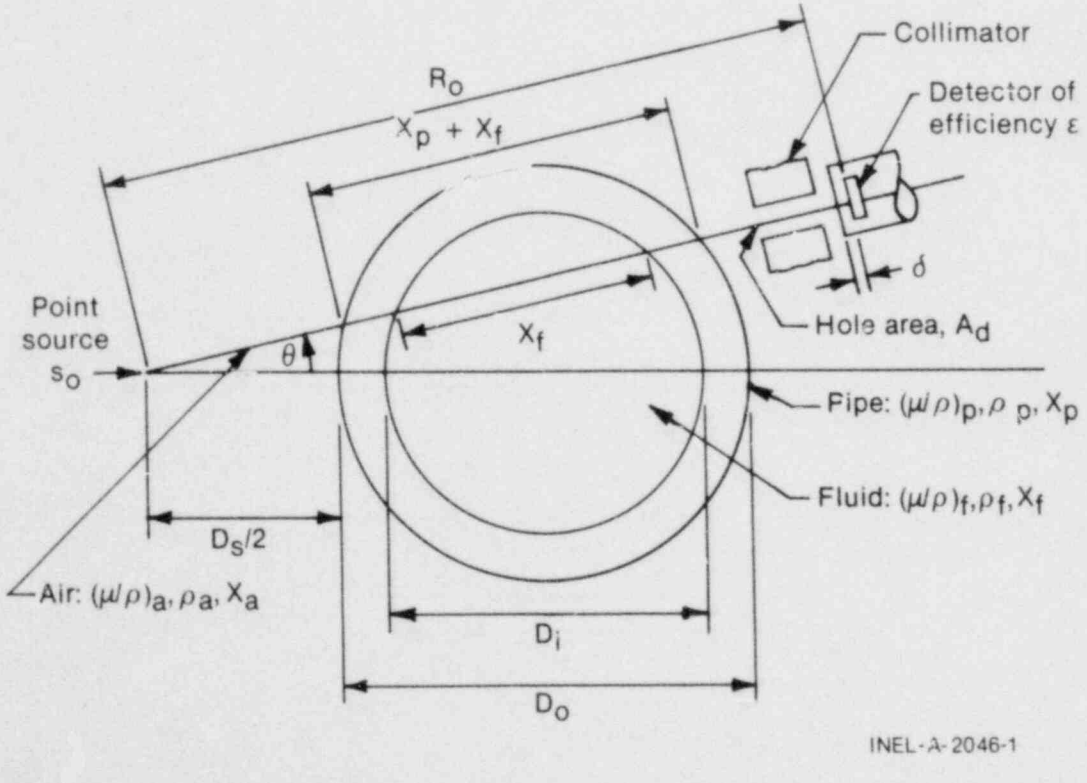

Figure 8. Geometry of scanning x-ray densitometer.

This slip ratio is included in the average density through the following relationship[a]

$$\bar{\rho}_{SLIP} = \frac{\left[\alpha S \rho_G + (1-\alpha)\rho_F\right]^2}{\left[\alpha S^2 \rho_G + (1-\alpha)\rho_F\right]} \qquad (13)$$

The average slip density as given by Equation (13) is used in Equation (1) to calculate the mass flow rate. However, the slip ratio of the individual phase velocities must be known. In a two-phase test loop (such as the air-water test facility) where the individual phasic mass flow rates input to the test section are known, the slip ratio can be directly calculated from conservation of mass, or

$$S = \frac{V_G}{V_F} = \frac{(1-\alpha)}{\alpha} \frac{\rho_F}{\rho_G} \frac{\dot{m}_G}{\dot{m}_F} \qquad (14)$$

In certain air-water data reported, this slip ratio will be used to show the effect on the measured two-phase mass flow rates. When a drag device is being used for a mass flow measurement during a transient type test (such as a Semiscale or LOFT LOCE), then the individual mass flow rate of the phases is not known. For this type of situation, a correlation of some type is required to obtain the slip ratio. One correlation that has proven to be moderately successful is the Hughmark and Pressburg holdup correlation,[8] from which the slip ratio can be obtained as a function of the void fraction, phase densities, total mass velocity, viscosity, and surface tension.

The Hughmark-Pressburg correlation for the slip ratio can be used with a drag coefficient correlation (from the previous section) in an iterative scheme to arrive at the two-phase mass flow rate.

a. Equation (13) can be obtained by combining Equations (1), (9), and (14) and solving for the average density.

3. AIR-WATER TEST RESULTS

A comprehensive testing program in steady-state, air-water mixtures was initiated to investigate the performance of various drag device configurations and to assess the accuracy of the measurement technique. Currently, nine different full-flow drag devices have been tested in 550 different air-water mixtures. Results from part of this testing are presented in the following sections.

3.1 Facility and Test Description

An initial effort in the development of full-flow drag devices for use in measuring two-phase mass flow was an extensive testing program in an air-water test loop. This program consisted of testing of several different drag devices for use in 6.67 cm ID piping, a drag device for use in the core inlet of the Semiscale Mod-3 vessel, and a hinged multihole drag plate for use in 3.40 cm ID piping. Results from the air-water testing were used to characterize the full-flow drag devices and to determine how accurately the mass flow rate of a two-phase mixture can be measured by using a full-flow drag device in combination with a densitometer.

The two-component (air-water) flow tests were performed in the Semiscale air-water test facility. The facility consists of a centrifugal pump, separation tank, air-water mixer, heat exchanger and associated valves, pressure and temperature measurement instrumentation, and reference turbine flowmeters necessary to calculate individual mass flow rates of air and water before mixing. All tests were conducted in either horizontal 6.67 cm ID piping or in horizontal 3.40 cm ID piping with the drag device downstream of the densitometer. The densitometer was mounted approximately 75 pipe diameters (125 pipe diameters in the case of 3.40 cm ID. piping) downstream of the air-water mixer and an instrument washer containing the drag device was mounted downstream of the densitometer. The general test procedure was to set up a flow condition and then to collect data during a 16-s sample period consisting of 3680 actual samples per data channel. The data were later processed to reduce the 3680 measurement samples to a single average data point (assuming steady-state conditions). The flow rates of air and water were independently varied from 0 to 0.40 kg/s for the air and from 0 to 8.45 kg/s for the water; these flow rates provided a range of void fraction, α, from 5 to 99.9% and covered all flow regimes.

3.2 Comparison Method

For ease in comparing the results of the mass flow measurements using the various drag devices, a normalized standard deviation of the measured mass flow rate was calculated from the known mass flow rate (or reference) input into the test section. This standard deviation can be expressed as

$$\sigma = \left\{ \frac{1}{N-1} \sum_{i=1}^{N} \left[\frac{(\dot{m}_{model})_i - (\dot{m}_{reference})_i}{\dot{m}_{max}} \right]^2 \right\}^{1/2} \quad (15)$$

where

N = the number of two-phase test points

$\dot{m}_{model}$ = the mass flow rate measured by the drag-density combination, Equation (1)

$\dot{m}_{reference}$ = the total of air and water mass flow rates input to the test section

$\dot{m}_{max}$ = the full-scale (maximum) mass flow rate that can be measured before electronic or mechanical saturation of the drag force transducer (all-water case).

3.3 Test Results

Test results are presented in the following sections from air-water tests of eight different drag devices for obtaining the mass flow rates of two-phase mixtures. Drag devices tested include the following: a drag disc, a drag screen, five multihole drag plates (four different configurations for 6.67 cm ID piping and one configuration for 3.40 cm ID piping), and a drag lattice.

3.3.1 Drag Disc. A drag-disc flowmeter historically had been used as a standard flow measurement instrument in the Semiscale Mod-1 system. As a basis for comparison between the historical measurement method and the full-flow drag devices that were being developed, a set of air-water tests was performed using the drag disc. Figure 9 is a photograph of the tested instrument. This device consists of a strain-gauged, cantilever beam, with a target mounted on one end that protrudes into the fluid flow. The force due to the fluid drag on the target is translated into a directly proportional output voltage, which is in turn converted to momentum flux using a calibration constant for the particular target. Figure 10 shows the results[a] from using the drag disc in combination with the two-beam gamma densitometer for measuring the two-component mass velocities at the test section versus the reference (or known) mass velocity input to the test section. The solid line shown in Figure 10 is the line of perfect fit, for which the measured and reference mass velocities are equal. A large amount of scatter is observable in the data. Part of the reason for this scatter is that the drag disc is only sampling a small local area of the flow (typically 11% of the pipe area); and for certain flow regimes, such as slug flows, the drag disc is not sampling areas of high momentum flux. However, during the Semiscale tests in which this device was used, the flow regimes were primarily homogeneous and the device would be expected to provide fairly accurate results. The normalized standard deviation for the 28 two-component test points taken was 11.2%. These results were obtained using a slip ratio of unity, a constant drag coefficient, and the density from the two-beam gamma densitometer.

a. Results from the air-water testing are shown separated by flow regime. In some cases, this information was obtained from observations (an acrylic plastic section was provided for flow observation), and in others, the flow regime was determined from Mandhane's flow regime map as provided in Reference 8.

3.3.2 Drag Screen. The first of the prototype full-flow drag devices tested was a drag screen with a flow blockage of 19%, shown in Figure 11. The drag screen was fabricated from 0.051-cm wire on a grid spacing of 0.508 cm and supported by a ring of 6.99-cm inside diameter. The supporting ring was inset in the drag screen instrument washer and was maintained external to the flow. Three of the strain-gauged drag-disc flowmeters (with the target replaced by a connector pin) were used as force transducers to measure the total force on the screen due to the fluid drag. These three transducers were connected to the supporting ring of the drag screen at 120-degree separations.

This drag device was tested at 27 different steady-state, two-component flow rates, at mass velocities ranging from 150 to 2100 $kg/m^2 \cdot s$. Results from these tests are presented in Figure 12. These results demonstrate the significantly better measurements obtainable from using a full-flow type of drag device over those results obtained using a drag disc. The normalized standard deviation for the results using the drag screen was 4.7%, as opposed to a value of 11.2% using the drag disc, a significant improvement. The results were obtained with a slip of unity and a constant all-water drag coefficient.

3.3.3 Multihole (Large) Drag Plate. Among the prototype full-flow drag devices tested in air-water mixtures was a multihole drag plate with seven large holes (diameter of 2.13 cm) and three partial holes resulting in a flow blockage of 23%. This device was designed for use in 6.67 cm ID piping and is shown in Figure 13 in the instrument washer insert used for holding the device in place. Three force transducers, in the same configuration used for the drag screen, were used with this device for measuring the drag force. A later version of this drag plate, which was designed for the LOFT experimental program, is shown in Figure 14. The portion of the drag plate exposed to the fluid flow is essentially identical to the drag plate shown in Figure 13. The LOFT prototype uses a single force sensor with the entire sensor assembly contained within the pressure boundary and exposed to the environment. An eddy-current displacement transducer is used to measure the displacement of a dual-range, cantilevered beam.

The three-point drag plate was used in 80 different steady-state, two-component flows for measuring the mass velocities. Results from these

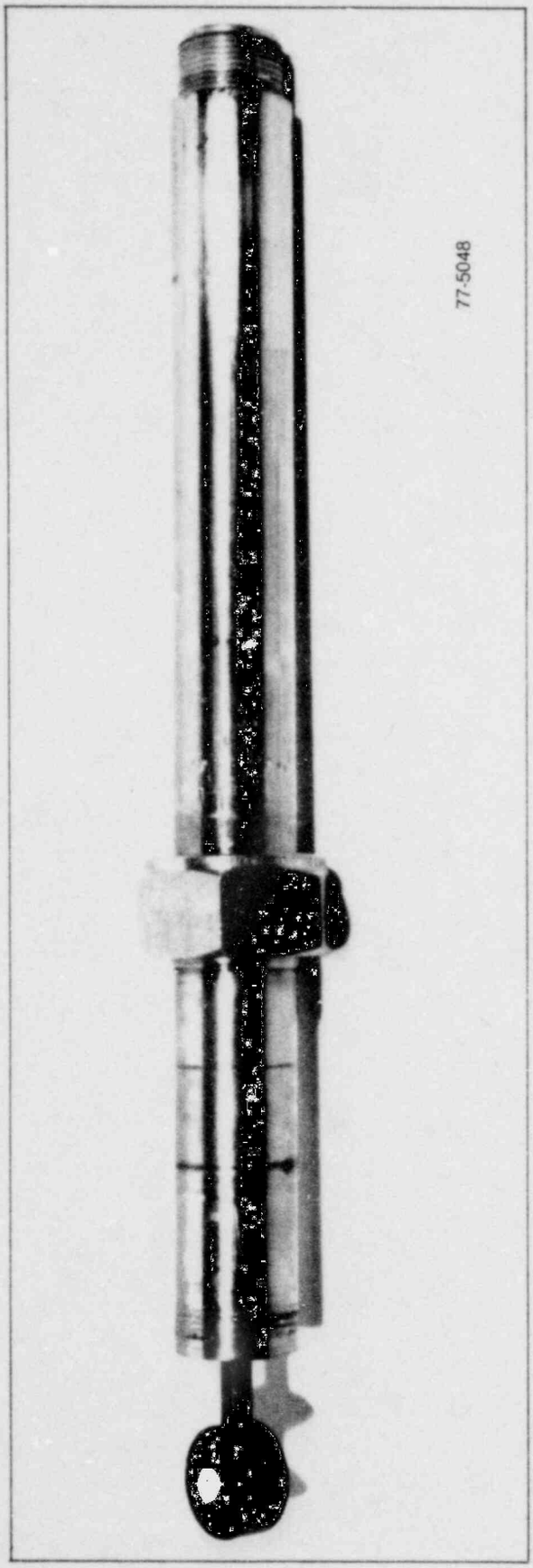

Figure 9. Drag-disc flowmeter.

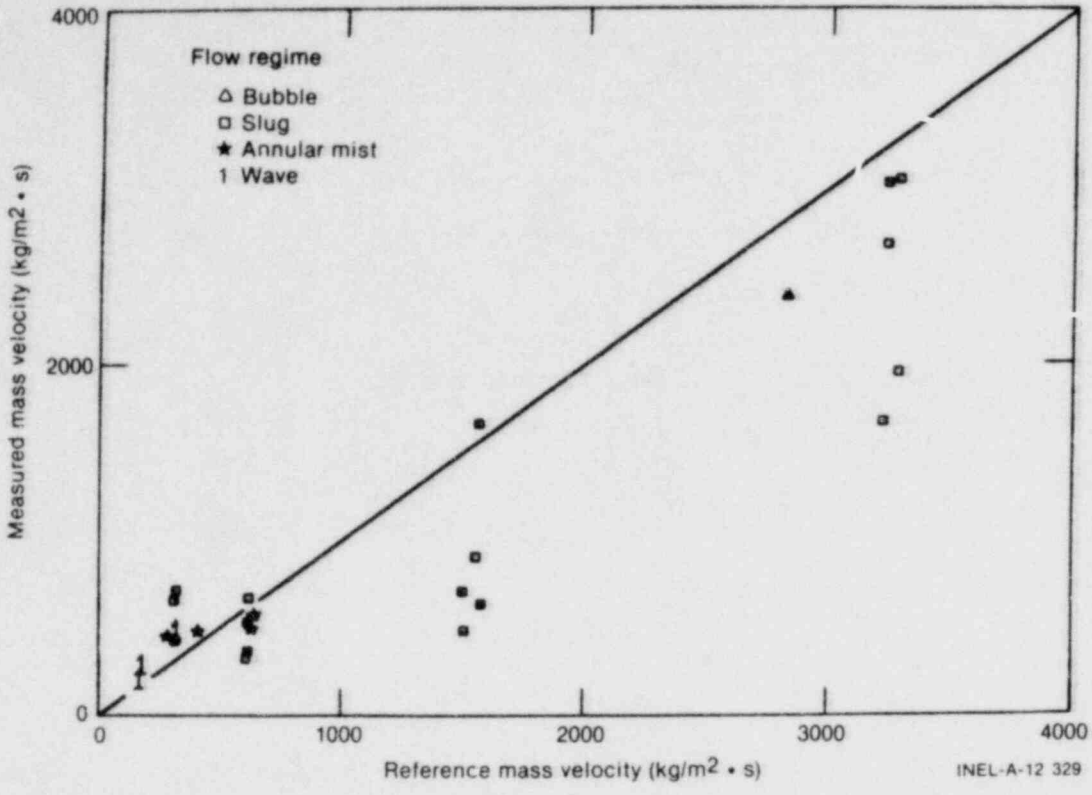

Figure 10. Typical mass flow measurement using drag disc in air-water mixture.

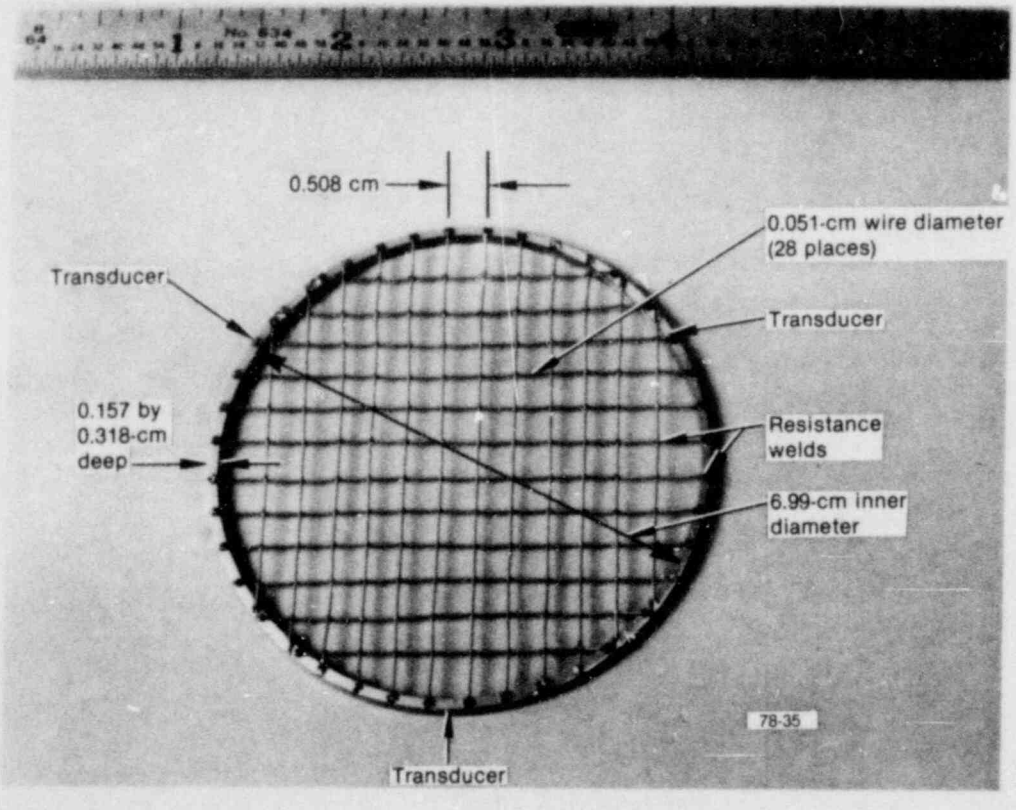

Figure 11. Prototype drag screen (three-point pickup). Flow blockage is 19% of pipe area.

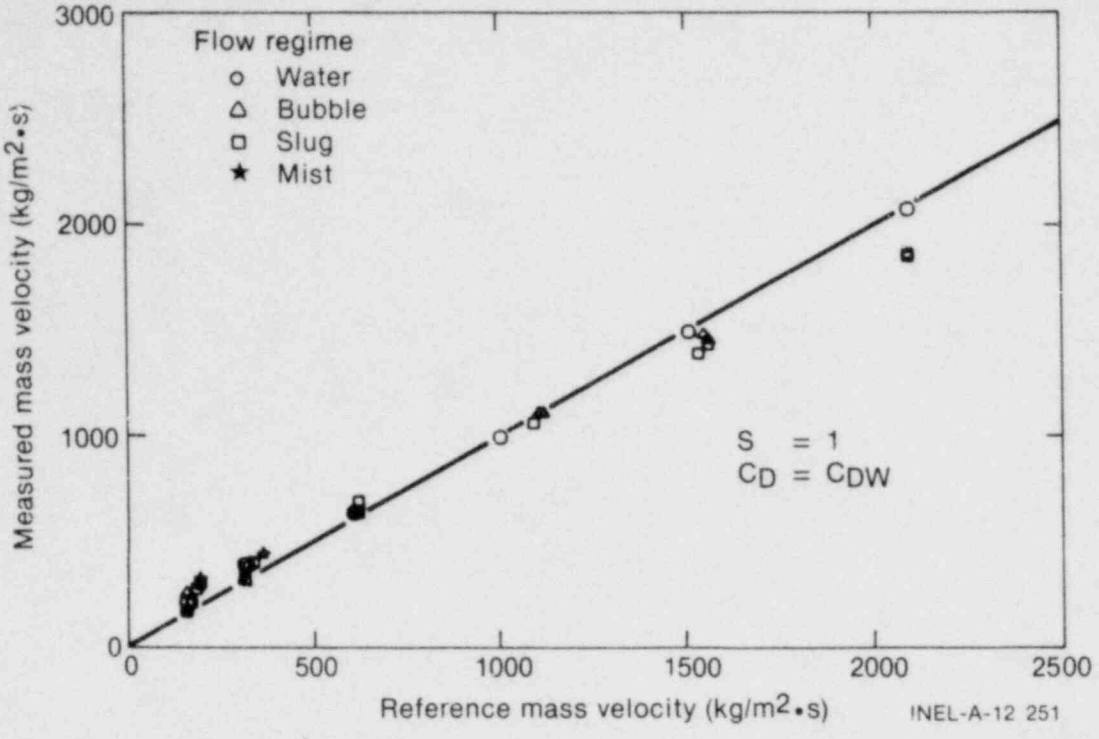

Figure 12. Mass flow measurement using a drag screen in 6.67 cm ID piping. Slip of unity and C_D = consta

tests are shown in Figure 15. The measured mass velocities are in better agreement with the reference mass velocities than with the results from using the drag screen. This configuration proved to be the most accurate of the drag devices tested and results in a normalized standard deviation of the mass velocity of 2.6%.

As a checkout and evaluation of the LOFT prototype, a series of air-water tests composed of 37 two-component flows was performed. The results from this testing are presented in Figure 16. The same type of results are observed in this figure as were observed when the three-point drag plate was used, with a resulting normalized standard deviation of 2.5%. The agreement between the two different force measurement methods (a cantilever versus a three-point force measurement) is good.

3.3.4 Multihole (Small) Drag Plate. Another of the prototype multiholed drag plates tested was one with 19 small holes of 1.19 cm in diameter with a resulting flow blockage of 33%. This plate used the same three-point force pickup as the drag screen and the large hole drag plate. This small hole drag plate was designed for use in 6.67 cm ID piping and is shown in Figure 17 in the mounting sleeve used for testing in the air-water loop. This device was tested in a total of 65 steady-state, two-component flows with a resulting normalized standard deviation of 5.8%. The results from the two component experiments are shown in Figure 18. (The error in the measurement increases as the mass velocity increases.)

3.3.5 Hinged Multihole Drag Plate—6.7 cm ID Piping. For certain applications, a three-point force pickup on the drag device was not feasible. One application in which a three-point force pickup was not feasible was at the core outlet on the Semiscale Mod-3 vessel. For this application, a hinged, multihole drag plate utilizing a single force transducer was used. This application will be discussed in more detail under the section on applications. However, prior to installation of the drag device, it was tested in the air-water test facility. Figure 19 shows the drag device in the support assembly used during air-water testing. The device was tested in horizontal 6.67 cm ID piping with the hinge in a vertical direction (the transducer to the side). The total drag force on the plate was obtained by multiplying the force measured by the force transducer by a constant, which is a function of the plate geometry, as shown in Figure 1. In this method, the total drag force on the drag plate, due to the distributed dynamic pressure force of the fluid, is assumed to be centered on the plate centroid. If a sufficiently long straight section of piping occurs immediately upstream of the drag plate, such that

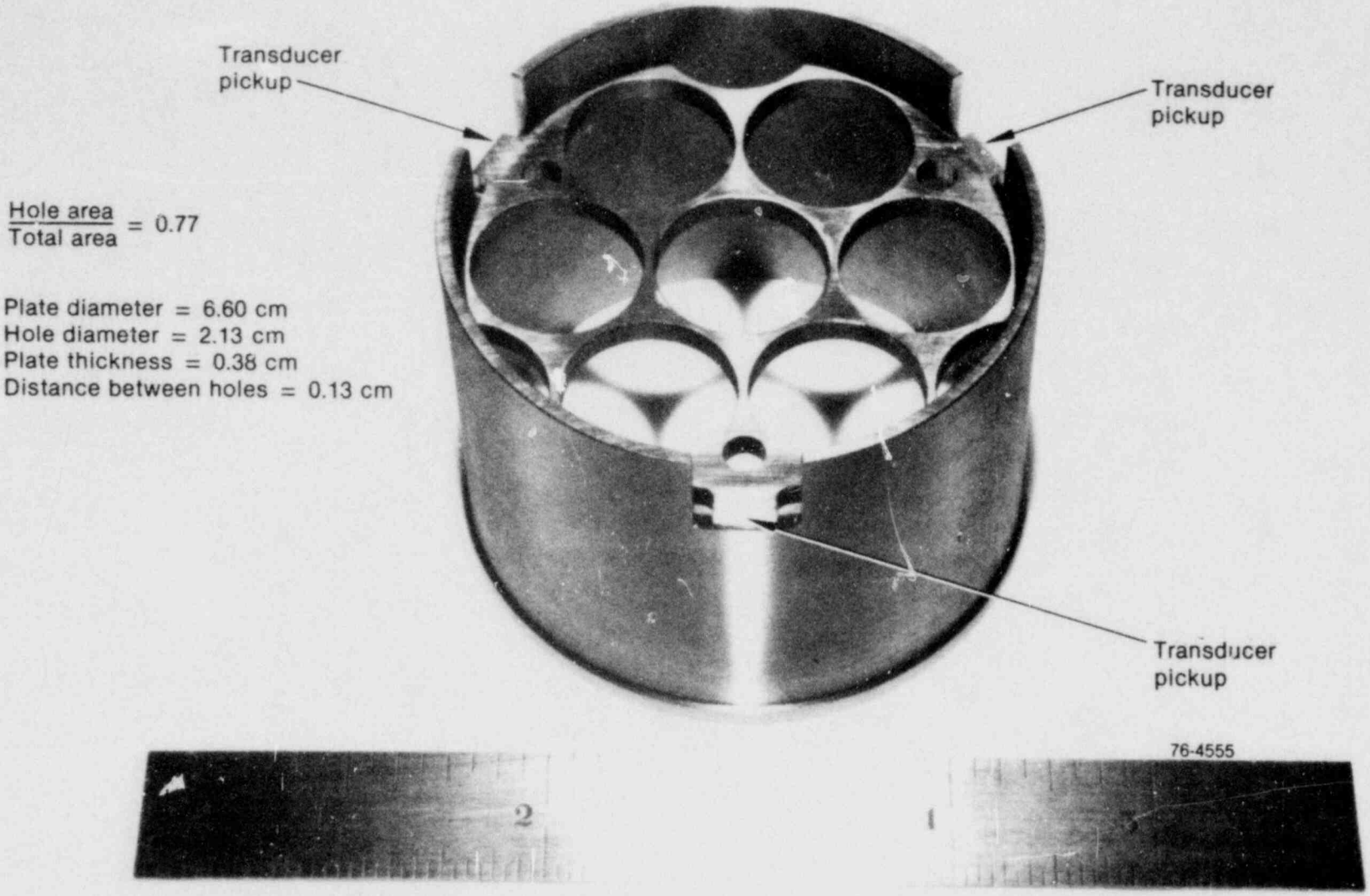

Figure 13. Multihole (large) drag plate shown in mounting sleeve with a flow blockage of 23% of pipe area.

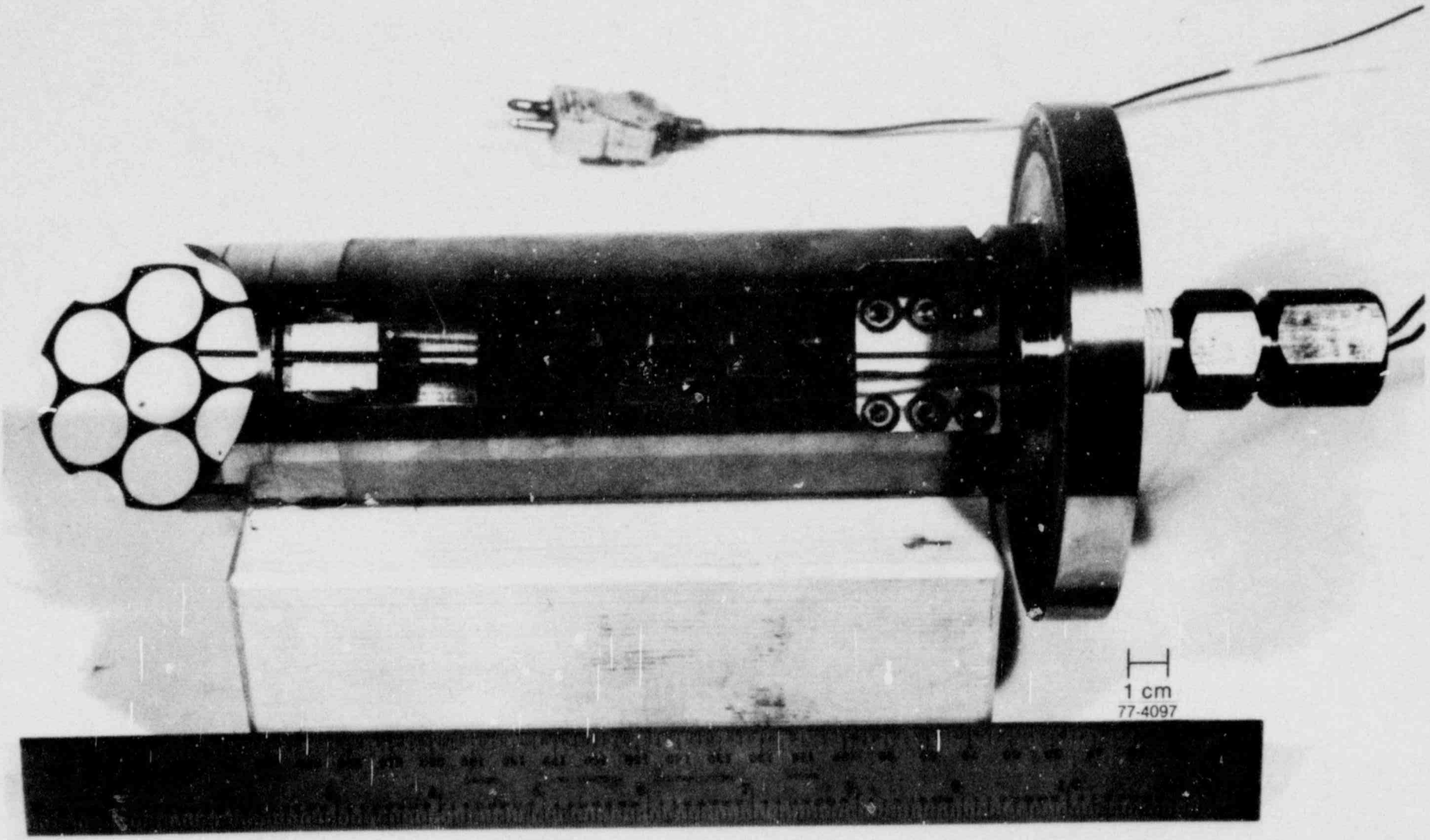

Figure 14. LOFT prototype drag plate—transducer assembly.

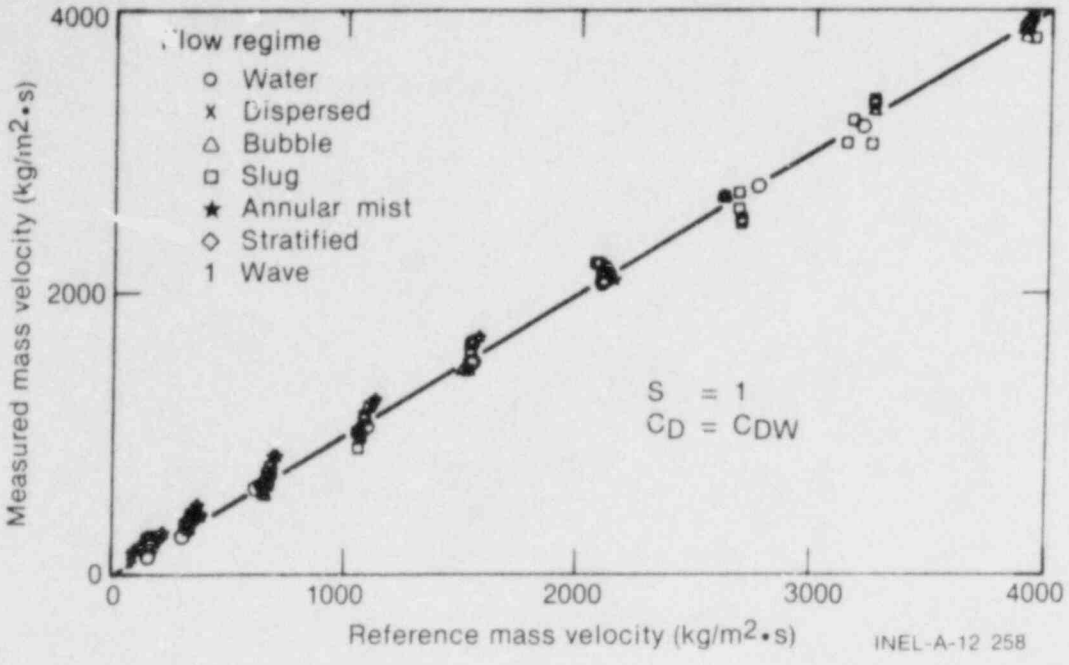

Figure 15. Mass flow measurements using the multihole (large) drag plate with three-point force measurement. Slip of unity and C_D = constant.

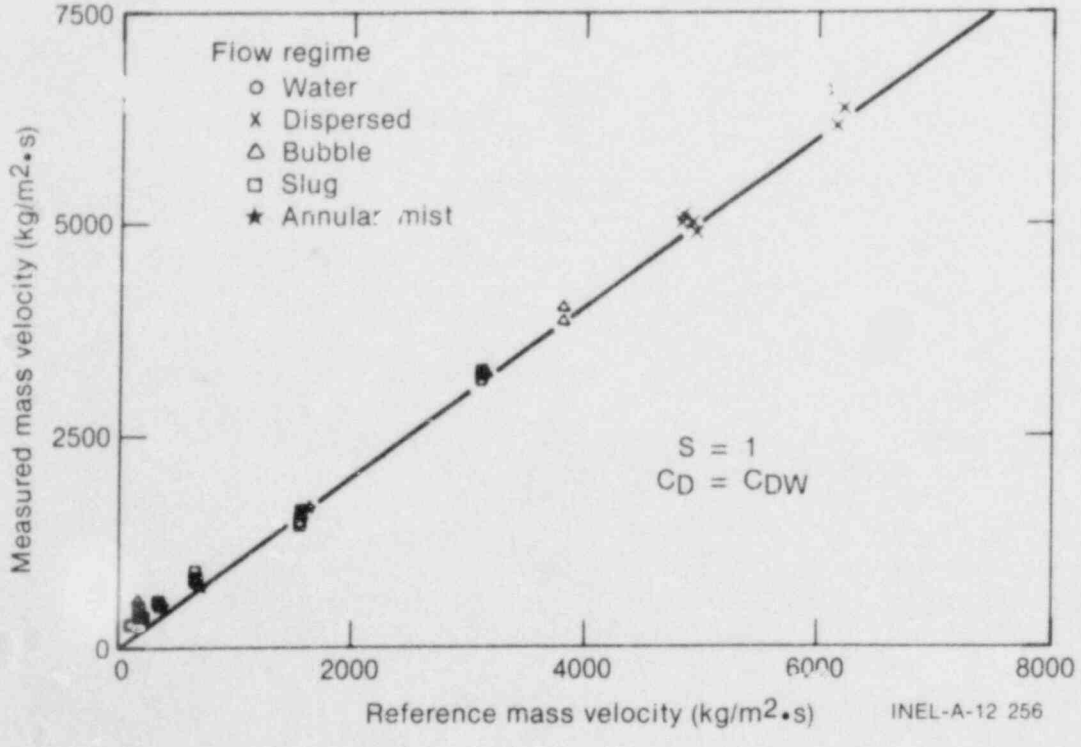

Figure 16. Mass flow measurements in air-water mixtures using the LOFT prototype multihole drag plate. Slip of unity and C_D = constant.

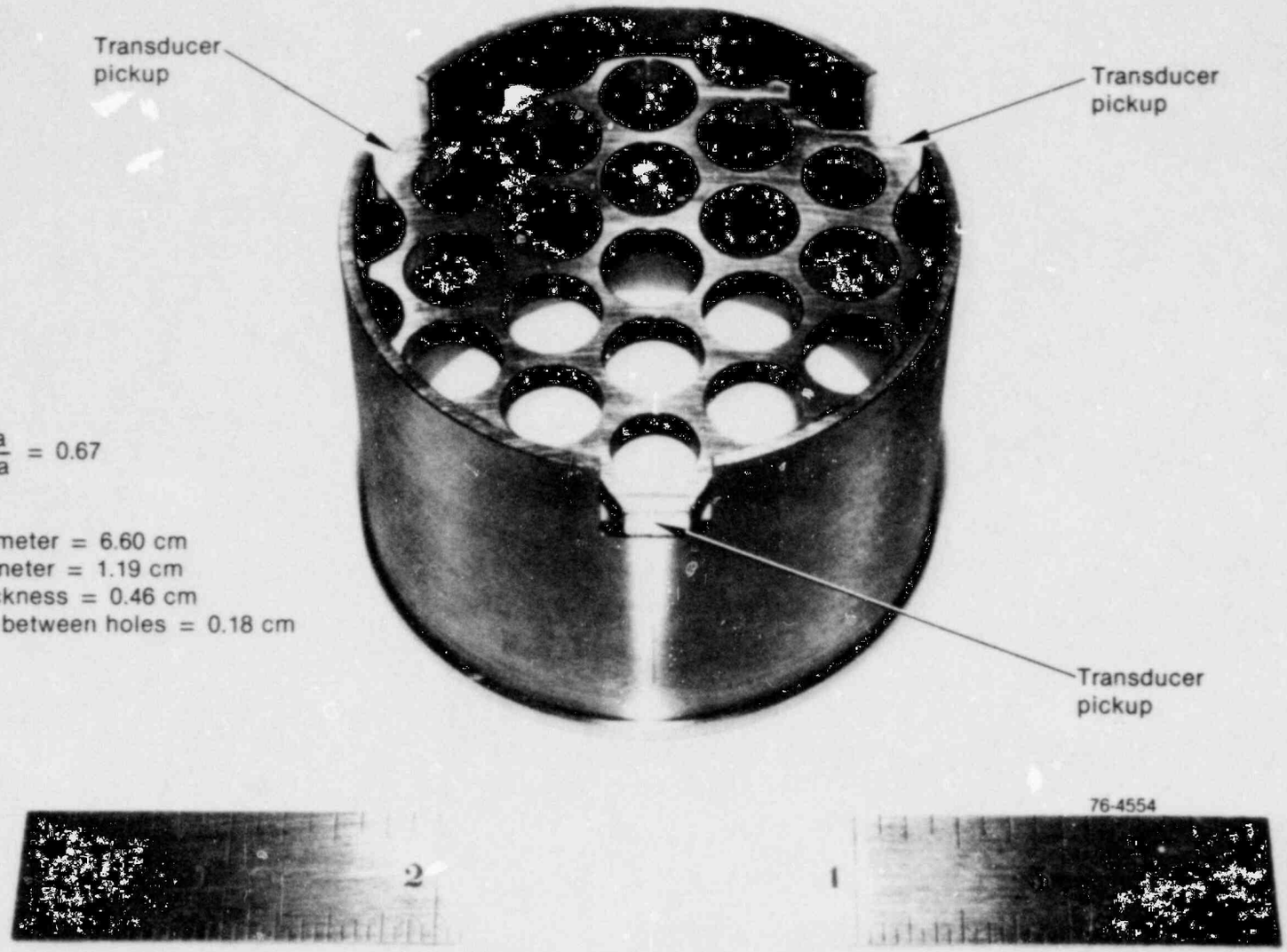

Figure 17. Multihole (small) drag plate shown in mounting sleeve, with a flow blockage of 33% of pipe area.

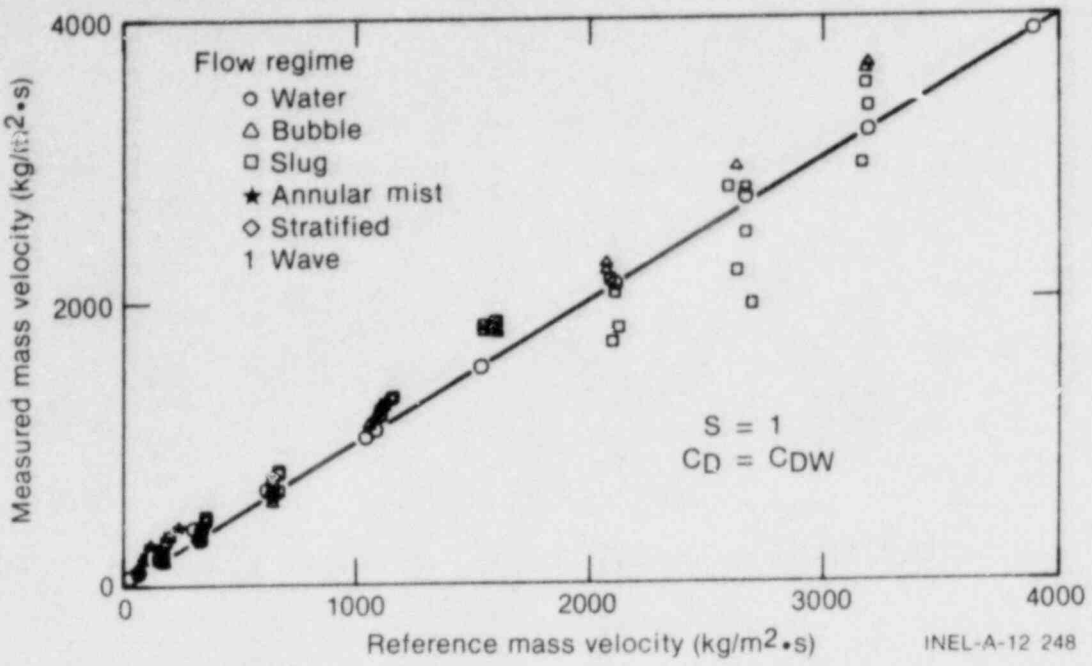

Figure 18. Mass flow measurements in air-water mixtures using the multihole (small) drag plate shown in Figure 17. Slip of unity and C_D = constant.

the flow is not disturbed, then this assumption should be valid. However, if a flow disturbance exists upstream (such as an elbow) which causes the two-phase flow profile to become skewed, then the total drag force obtained from this method will be in error. The size of the error would depend on the degree of skewness in the momentum flux profile, and no estimate of the error is currently available.

The application for which this device was intended (the Mod-3 core outlet) is in a vertical piping segment in which the possible skewness of the momentum flux profile is minimized. During the air-water testing, a straight section of piping of about 75 diameters in length was used upstream of the test section to eliminate any momentum flux profile effects due to upstream disturbances.

The portion of the drag device, which was exposed to the fluid flow, was very similar to the three-point, small-hole drag plate for which the results were discussed in the previous section. The major difference was that the holes in the hinged drag plate were beveled, such that there was a very small flat between holes (about 0.3 mm). The hinged drag device was tested in 35 different air-water mixtures; the results from the mass flow measurements are presented in Figure 20. This figure does not show as many errors as shown in Figure 18 for the unbeveled, three-point-pickup, drag device. The reason for this reduction in errors is not obvious. No difference should have occcurred due to the force measurement method (hinged versus three-point) because a long section of straight pipe was immediately upstream of the test section. In addition, a test series was performed using the small hole drag plate in which the holes had been beveled, and no difference in the results was found between the beveled and unbeveled holes. The normalized standard deviation for the beveled hinged drag device is 3.8%, compared with 5.8% for the unbeveled three-point-pickup, drag device. Assumptions used for the mass flow calculations were the same as for all previously discussed results (that is, S = 1, C_D = constant).

3.3.6 Hinged Multihole Drag Plate—3.40 cm ID Piping. A practical advantage of using a hinged drag device, instead of a drag device with a three-point pickup, is the cost savings in force transducers, supporting electronics, and data collecting channels. These considerations stimulated additional effort to design a prototype hinged drag device for 3.40 cm ID piping with an outside diameter for the drag device of 3.32 cm. Figure 21 shows the resulting drag plate, which has a flow blockage of 18%. This drag device was extensively tested in the air-water test facility, with the scanning x-ray densitometer used to provide the cross-sectional average void fraction for the mass flow

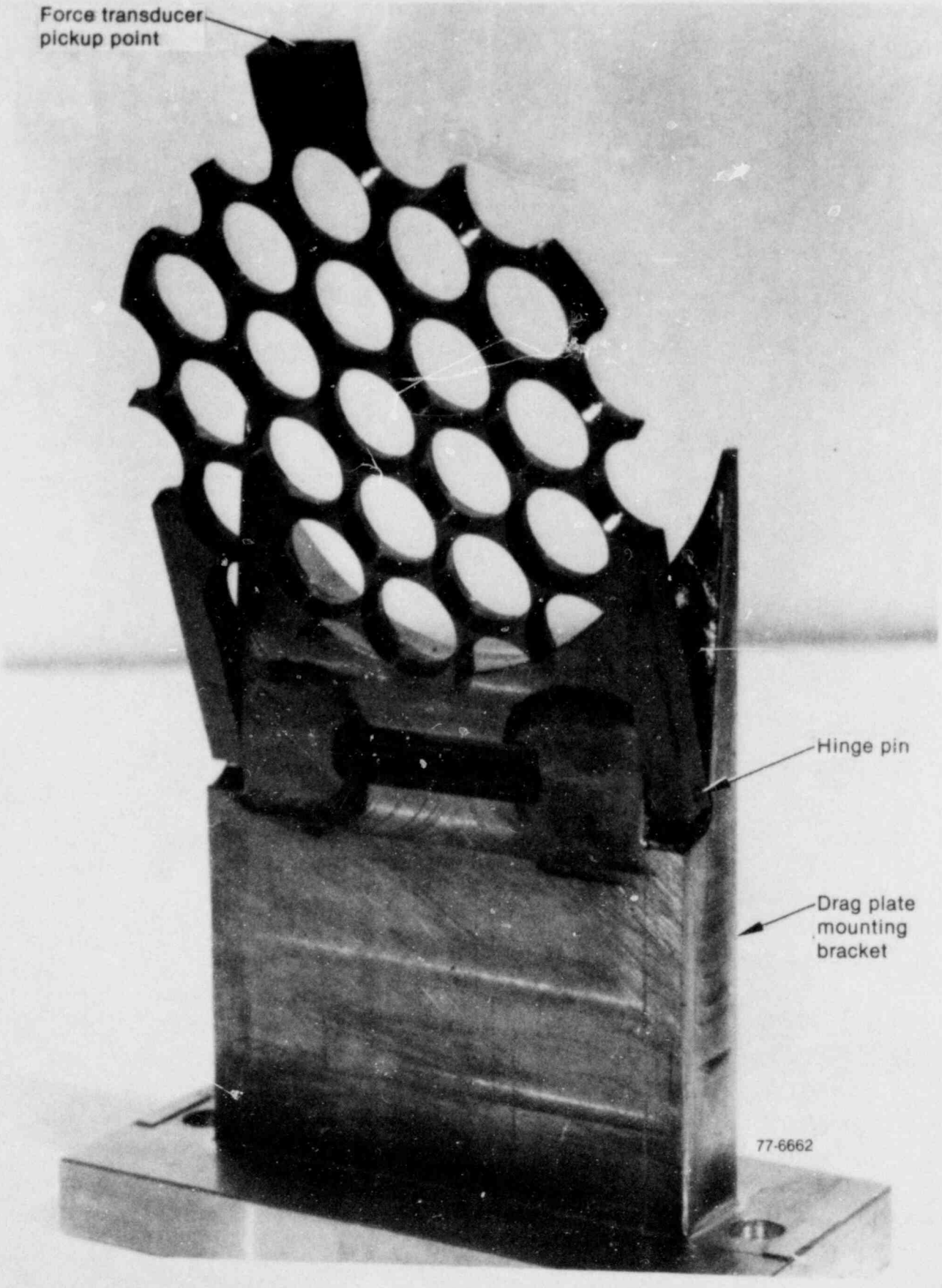

Figure 19. Hinged, multihole drag plate, used in the core outlet of the Semiscale Mod-3 vessel shown with support assembly for air-water testing. (Flow blockage of 34% in 6.67 cm ID piping).

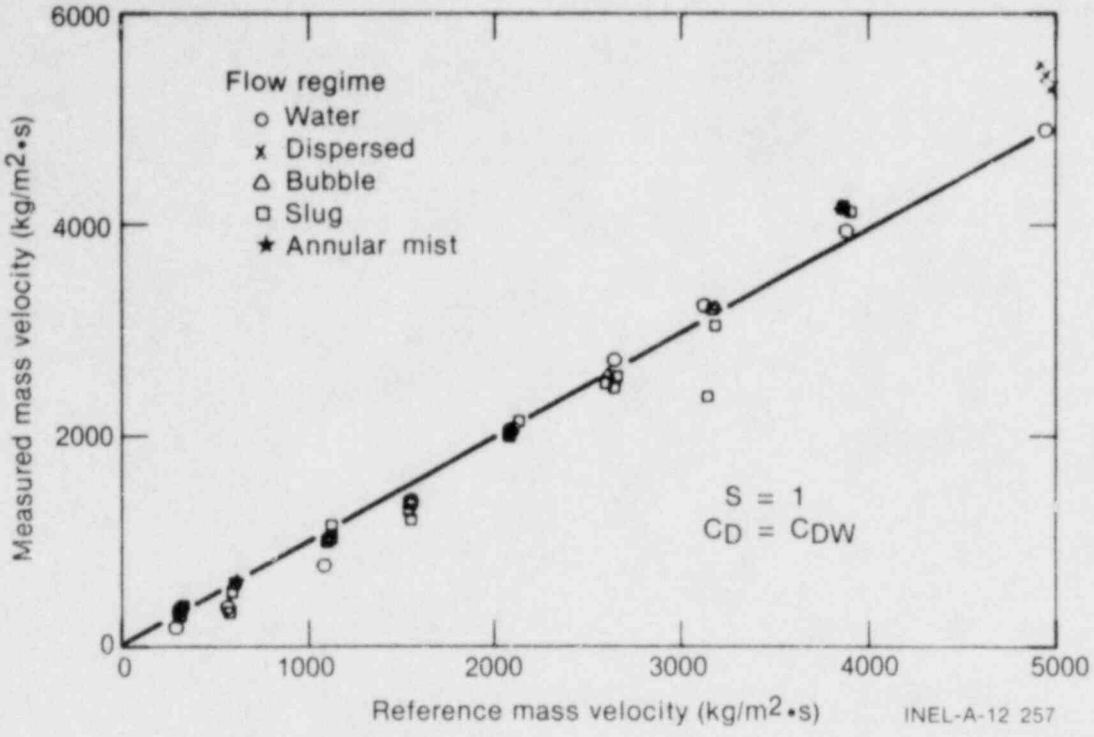

Figure 20. Mass flow measurements in air-water mixtures using the hinged drag plate in 6.67 cm ID piping. Slip of unity and C_D = constant.

measurements. Figure 22 presents the results from air-water testing of this drag device in 47 different two-component flows, comprised of annular mist flows. In this figure, the same homogeneous model was used as in the previous figures (that is, the slip was assumed to be equal to unity, and a constant drag coefficient e. al to the single-phase drag coefficient was assumed). The normalized standard deviation for these results is 4.2%.

Figure 23 presents results from the same data that were used for Figure 22, with the slip ratio of the phasic velocities included in Equation (13) for the cross-sectional average density. The values for the slip ratios were obtained from Equation (14) using the loop input mass flow rates and the void fraction from the scanning densitometer. This method provides a modest reduction in the errors for the annular mist flows, resulting in a normalized standard deviation of 3.3%.

Figure 24 shows the results from the same data using the Hughmark-Pressburg slip correlation[a] and a correlation for the drag coefficient obtained from a second-order polynomial fit to the data in Figure 5. These correlations improve the mass measurement significantly and reduce the normalized standard deviation from 4.2% with the homogeneous drag model to 0.5% using both correlations. These correlations have proven to be successful for annular mist flows and need to be extended to the other flow regimes.

3.3.7 Hinged Drag Lattice. One of the special applications for a full-flow drag device is at the core inlet to the Semiscale Mod-3 vessel. The core inlet is a difficult location to make a mass flow measurement as the bottom portion of the 25 electrically heated rods, used to simulate nuclear fuel rods, pass through the measurement location. The hinged drag lattice, shown in Figure 25, is the resulting design choice. The dra[illegible]e was fabricated from diamond-shape[illegible] 1.5 mm wide by 3.0 mm in height. Fo[illegible] air-water loop, a mockup of the cor[illegible]ction was fabricated including a single-bea[illegible]amma densitometer, collimated and aligned with the beam passing between two rows of the rods. This assembly was tested in both the vertical and horizontal orientations in the air-water loop. The horizontal ori[illegible]ntation was with both the hinge pin (with the force transducer to the side) and the densitometer beam vertical, passing between the

a. The Hughmark-Pressburg coefficient was used in combination with the air-water data to obtain a slip correlation using a quadratic fit to the data over a void fraction range of 0.85 to 0.999.

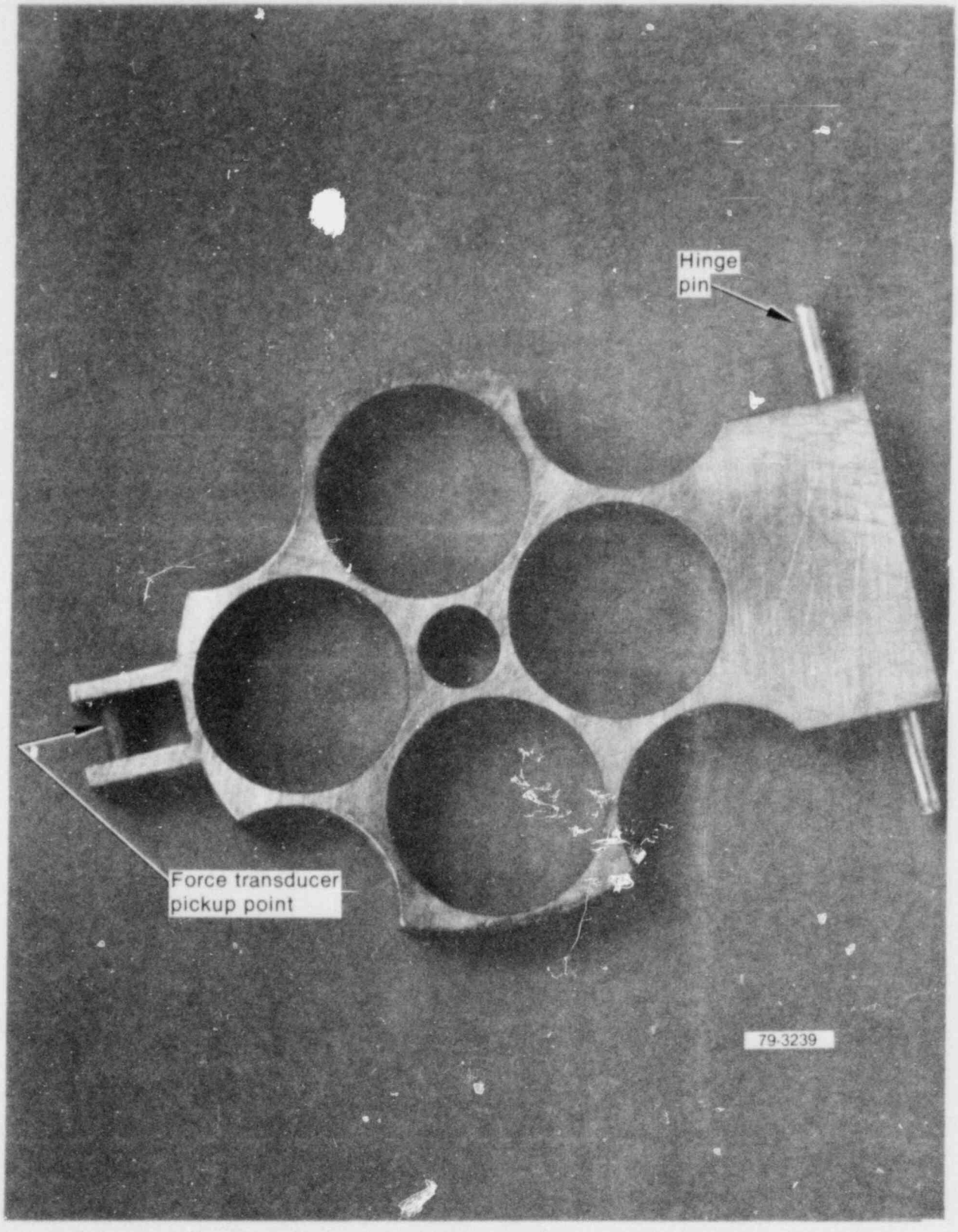

Figure 21. Hinged, multihole drag plate used in 3.40 cm ID piping.

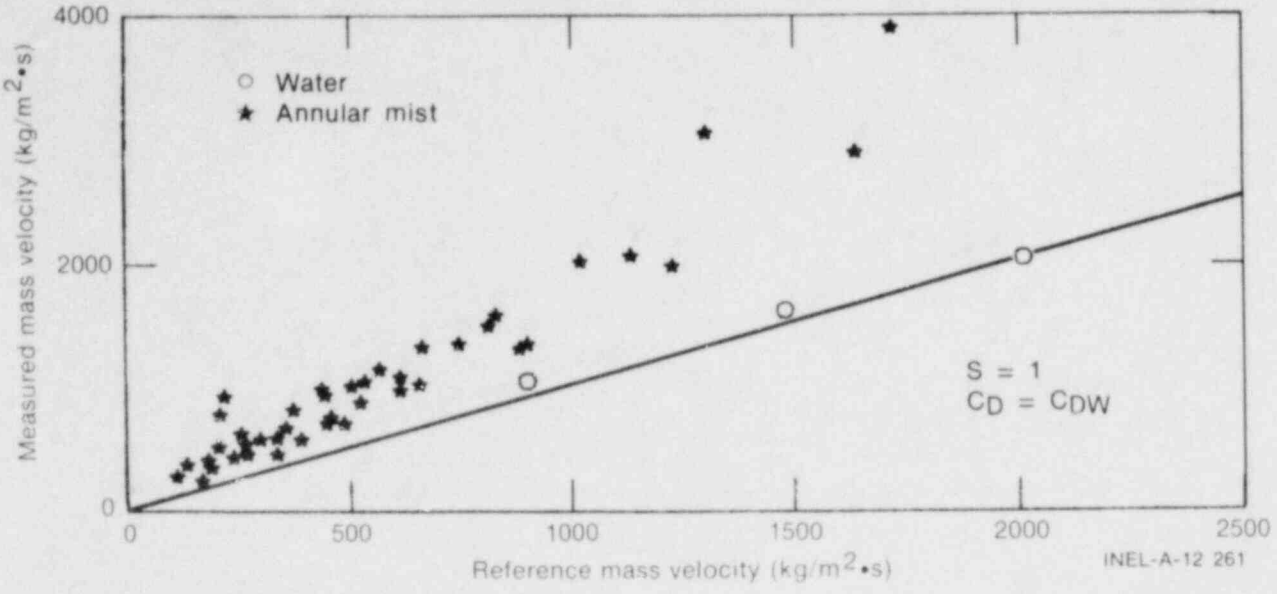

Figure 22. Mass flow measurements in air-water mixtures using the hinged, multihole drag plate in 3.40 cm ID piping. Slip of unity and C_D = constant.

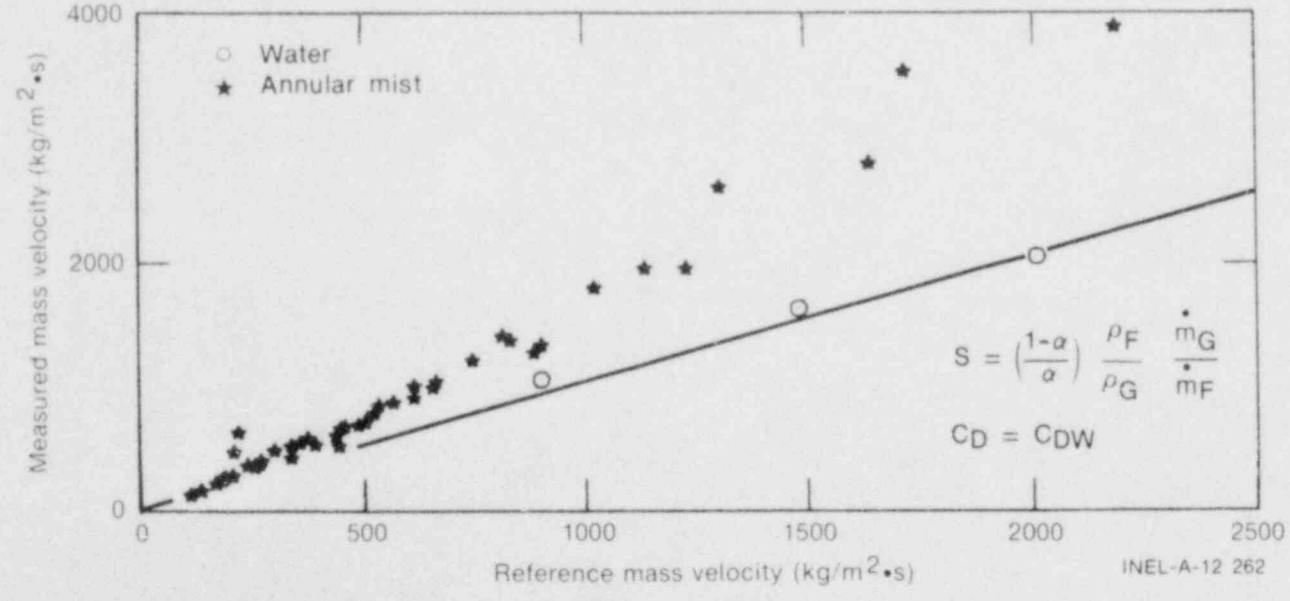

Figure 23. Mass flow measurements in air-water mixtures using the hinged, multihole drag plate in 3.40 cm ID piping. Results include the effect of slip between the phases.

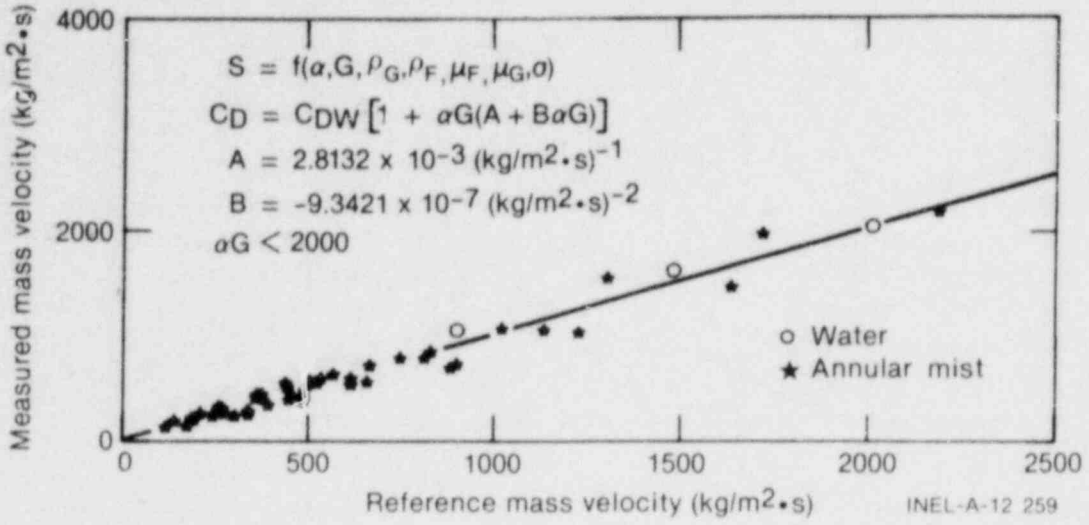

Figure 24. Mass flow measurements in air-water mixtures using the hinged, multihole drag plate in 3.40 cm ID piping. Results include Hughmark-Pressburg correlation for the slip and the correlation on the basis of the αG parameter for the drag coefficient.

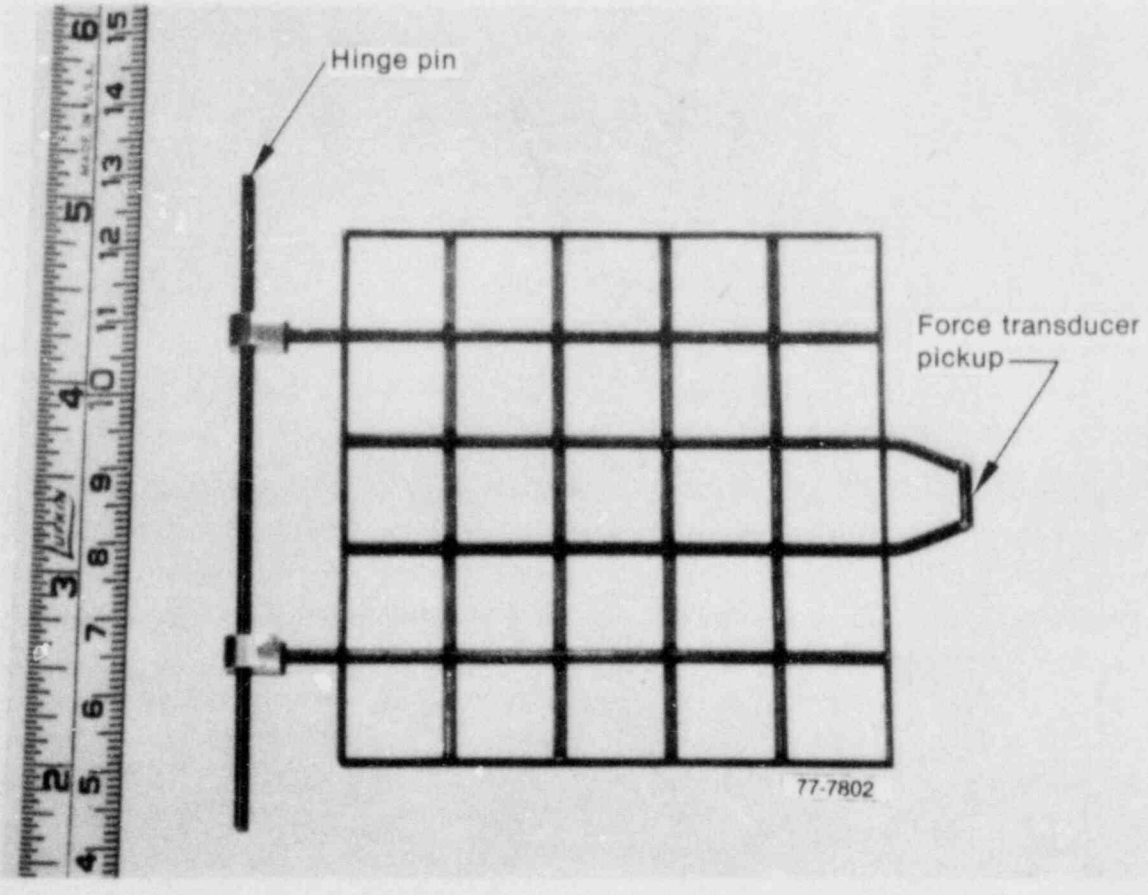

Figure 25. Hinged drag lattice for use in the core inlet of the Semiscale Mod-3 vessel.

second and third rows of rods. The horizontal tests were performed for direct comparison to other testing that had been performed. The results from testing in 35 air-water mixtures are presented in Figure 26. The measured mass velocities were calculated using the measured beam density as the average density and a constant drag coefficient obtained from all water calibration flows. Considering the crude density measurement, the results are exceptionally good with a normalized standard deviation of 1.2%.

3.4 Summary—Air-Water Test Results

The air-water tests were intended to characterize the various full-flow drag devices and to determine with what accuracy the mass flow rate of a two-phase mixture could be measured by using a full-flow drag device in combination with a densitometer. The air-water testing fulfilled these objectives, in addition to pointing out potential problems and areas in which further work is needed. A full-flow drag device was found to result in considerable reduction in measurement errors over those resulting from the use of a local device, such as a drag disc. Table 1 provides a summary of all reported air-water test results. Further, all other factors being equal, a multihole plate provided better measurements than a screen. However, the flow blockage caused by the drag device appears to be as important as the type of full-flow drag body. The optimum design for a full-flow drag device appears to be one in which the flow blockage is the minimum possible, while allowing the entire flow to be sampled and sufficient structural strength to be maintained.

For a multibeam gamma densitometer, over all the flow regimes, the particular analytical model used for obtaining the cross-sectional average density from the chordal-averaged beam densities was found not to be particularly important in the final results. The effect of the phasic slip was found to be of secondary importance when considered over

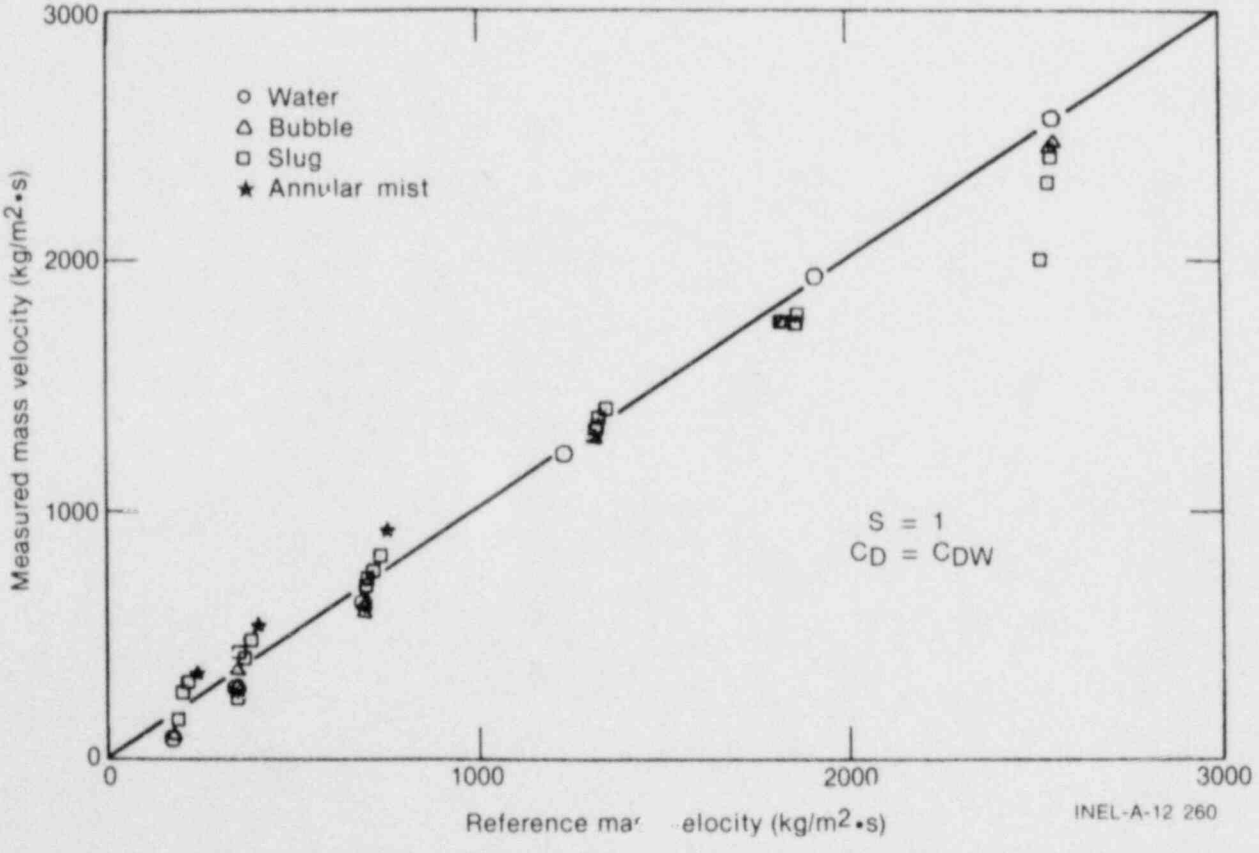

Figure 26. Mass flow measurements in air-water mixtures using the hinged drag lattice shown in Figure 25. Slip of unity and C_D = constant.

Table 1. Results from Air-Water Tests of Drag Devices

Drag Device	Normalized Standard Deviation (%)	Flow Blockage (%)
Drag disc	11.2	11
Drag screen	4.7	19
Large multihole plate		
three-point	2.6	23
LOFT prototype	2.5	23
Small multihole plate	5.8	33
Hinged multihole plate		
6.67 cm piping	3.8	34
3.40 cm piping		18
Homogeneous model	4.2	
Slip model	3.3	
Model with S & C_D correlations	0.5	
Drag lattice	1.2	34

all of the flow regimes. For annular mist and stratified flow regimes where the slip ratio may be large (3 to 15), the effect may be as significant as 30% of the mass flow rate measurement. The most important of the considerations in making a drag-density combination mass flow measurement is the effect of the various flow magnitudes on the drag coefficient. For high velocity annular mist flows, this effect could produce errors of 200% of the actual mass flow reading. Additional work is required for understanding and accounting for this two-phase effect on the drag coefficient. To obtain better drag coefficient correlations will require a better analytical model than the two-velocity model used in this report for calculating the two-phase momentum flux.

4. TRANSIENT STEAM-WATEP TESTING

A series of transient steam-water tests was peformed in the LOFT Test Support Facility (LTSF) Blowdown Loop for testing the LOFT prototype drag plate (shown in Figure 14). The purpose of these tests was to assess the transient performance of the drag plate under saturated fluid conditions and to determine with what accuracy the mass leaving the system could be measured. A comprehensive description of this testing has been detailed in a previous report.[4] Therefore, only a brief description of the facility and test results from the partial blowdowns are provided here.

4.1 Facility and Test Description

The Blowdown Loop at LTSF is a small-scale assembly designed for experimental investigation of measurement and component response in an anticipated PWR steady-state or transient environment. The main pressure vessel is constructed of 40.60 cm ID Schedule 160, 316 stainless steel pipe. The vessel has an approximate volume of 0.28 m^3. Pressure is maintained with a nitrogen head over the vessel fluid. The circulating pump is a volute-type centrifugal pump rated for a nominal flow of 0.011 m^3/s at a total head of 60 m of water. Heat input is from two heater rods and the pump. An isometric view of the facility appears in Figure 27. The drag plate instrument location is indicated.

To obtain transient conditions, the quick-opening blowdown valve (QOBV) on the end of the blowdown leg is activated. With the appropriate system valves opened or closed, both complete and partial blowdown transients are possible. In a complete blowdown transient, the entire system is vented to the atmosphere. In a partial blowdown transient, the pressure vessel is valved out of the system and only the piping is allowed to blow down.

In a typical experiment, the facility operating temperature and pressure were 503 K and 10.34 MPa. The blowdown leg was maintained at 425 K so that the Teflon seals in the QOBV would endure more than one test. The blowdown leg constitutes a major portion of the mass in the system for the partial blowdown configuration. For this reason, the initial conditions for the partial blowdowns should be considered to be 425 K and 10.34 MPa.

The data from all flow measurement transducers were recorded on analog tape by an Ampex 3000 tape recorder. These data were later digitized at 50 samples per second and reduced to momentum flux and mass flow measurement on the CDC 7600 computer. A slip ratio of unity and a constant all water drag coefficient were used for data reduction.

4.2 Partial Blowdown Results

Four partial blowdown experiments were conducted. The transient flow characteristics can be observed in the results of a typical blowdown in Figure 28. (The blowdown was initiated at 0.12 s.) Examination of the density traces showed an initial period of near homogenity lasting for about 1.5 s; then a period of slugging, or large amplitude waves, lasting for the next 3 s; and finally, a period of low-frequency, wavy stratified flow, ending in all steam at approximately 11.2 s when the QOBV was closed.

As can be seen in Figure 28, the time response of the drag plate is quite fast; there is no evidence of ringing even though the system is lightly damped.

The results of integrating the mass flow rate as measured by the drag plate over the duration of the test for the four partial blowdowns appear in Table 2. The value of total system mass also appears in Table 2. Examination reveals that the drag plate-densitometer combination measures the integrated mass flow within about 10%, assuming the upper mass limit to be the actual value.

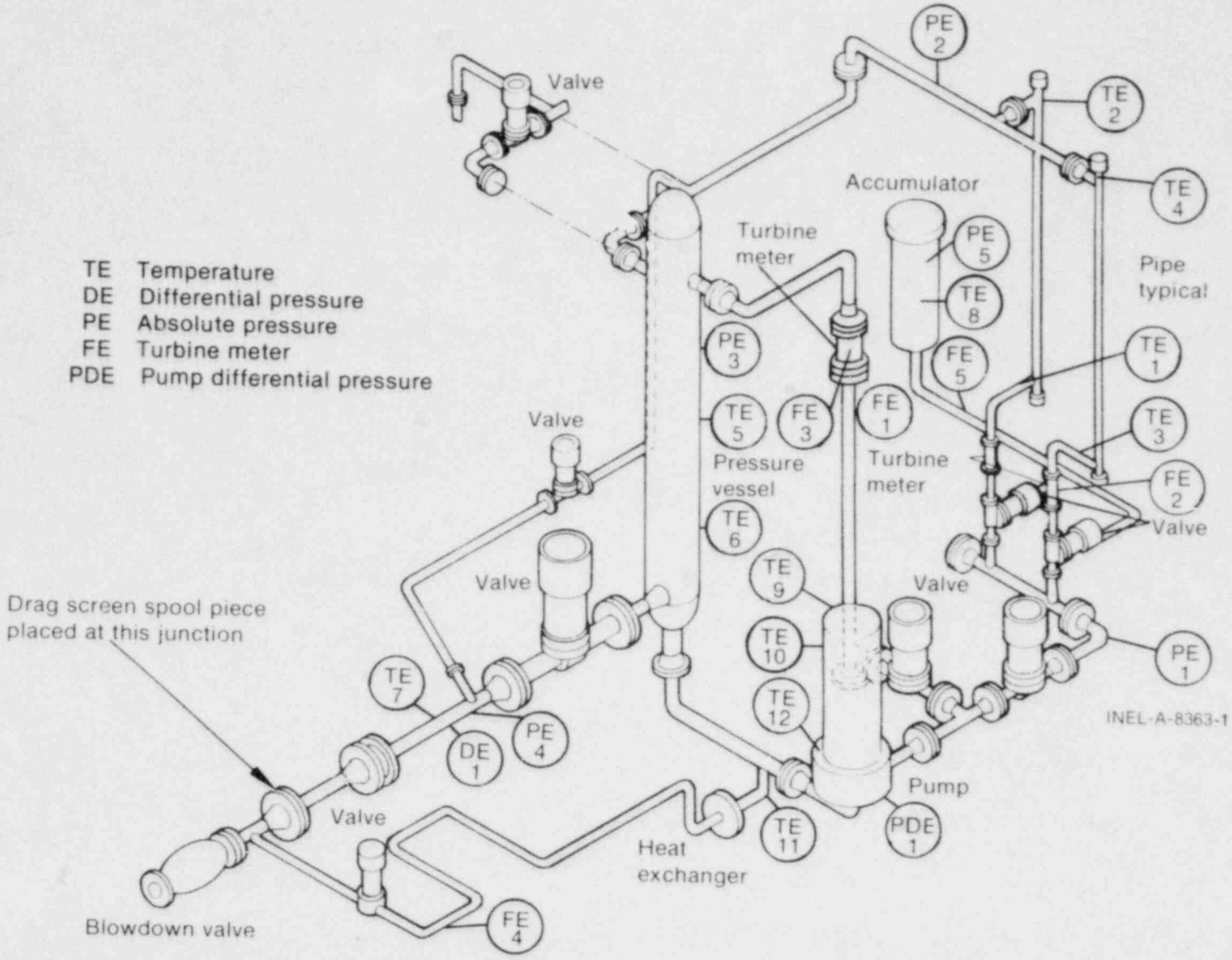

Figure 27. Isometric view of blowdown loop in LTSF.

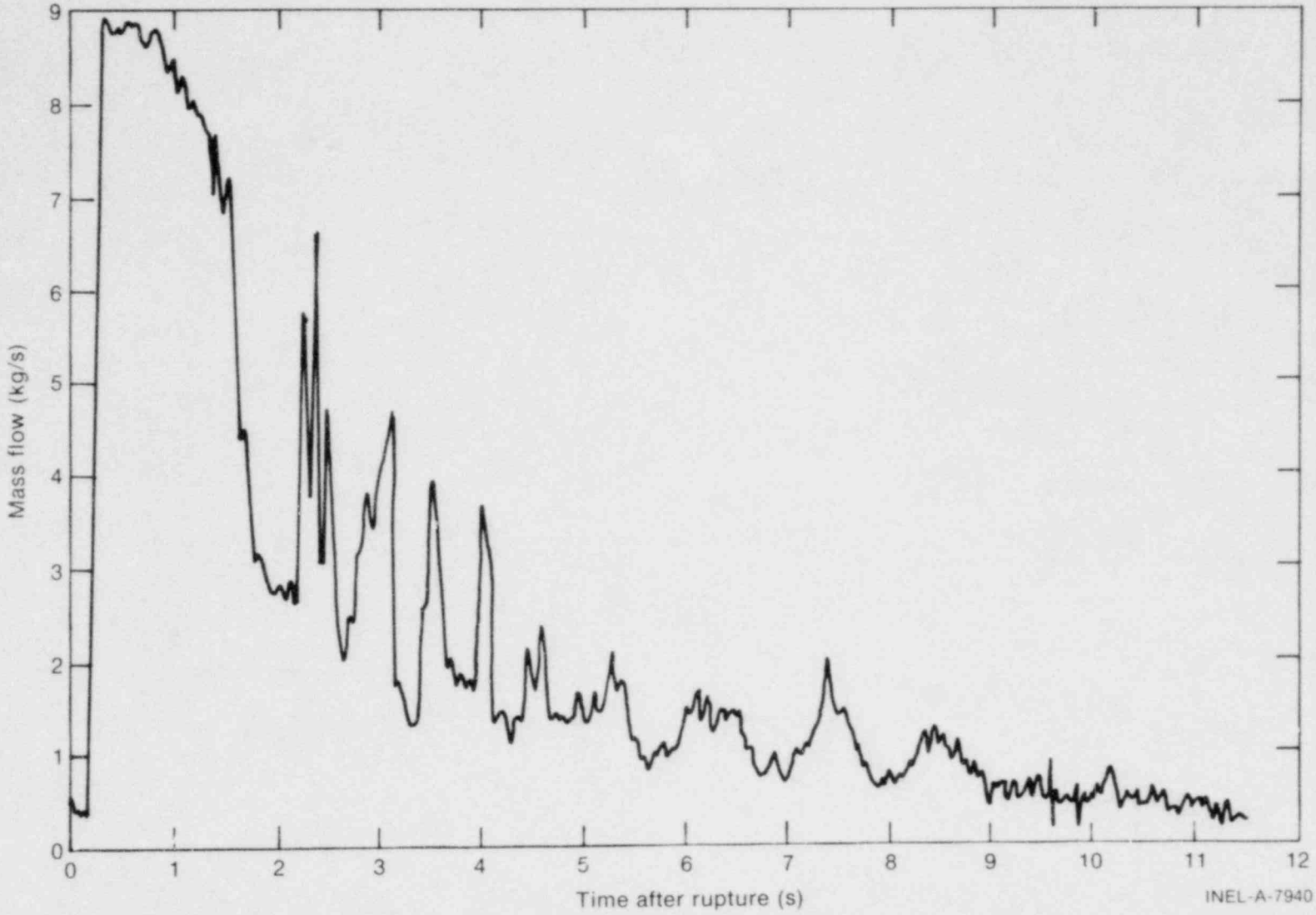

Figure 28. Mass flow calculated from drag plate and gamma densitometer during partial blowdown.

Table 2. Total System Mass for the Partial Blowdown Configuration and Measured Mass Flow Values

	Time Integrated Mass Flow (kg)	
Blowdown	Measured Value	Upper Limit Error (%)[a]
1	27.7	7.7
2	27.38	8.8
3	27.8	7.4
4	26.9	10.4

a. Mass expelled during blowdown:

Maximum = 30.03 kg

Minimum = 27.69 kg.

5. APPLICATIONS—SEMISCALE MOD-3

The Semiscale Program[9] is a continuing series of thermal-hydraulic experiments to generate data that can be applied to the development and assessment of analytical models that describe transient phenomena in water-cooled nuclear power plants. Emphasis is placed on acquiring integral system effects data that characterize the most significant thermal-hydraulic phenomena likely to occur in the primary coolant system of a nuclear plant during the depressurization (blowdown) and ECC phases of a LOCA. The experiments are performed with a test system that simulates the principal features of a nuclear plant but that is smaller in volume. Nuclear heating is simulated in the experiments by a core composed of an array of electrically heated rods, each of which has dimensional and heat flux characteristics similar to those of a nuclear fuel rod.

The Semiscale Mod-3 test program is being conducted to investigate the thermal and hydraulic phenomena accompanying a hypothesized LOCA in a water-cooled nuclear reactor system. The Semiscale Mod-3 tests are conducted in a two-loop system with both intact and broken loops containing active components representative of nuclear system components. The Mod-3 vessel is designed to be representative of a PWR, using an upper head injection emergency core cooling system. The Mod-3 vessel uses an external pipe to represent the downcomer annulus of a PWR. An isometric view of the Semiscale Mod-3 system is provided in Figure 29.

5.1 Drag Device Locations

The locations and types of all drag devices in the Semiscale system are provided in Table 3. The following brief descriptions of the devices are provided to familiarize the reader with the various types.

5.1.1 Guide Tube. In the upper head of the Mod-3 vessel is a tube with a 1.6-cm inside diameter meant to simulate a guide tube of a PWR. A drag device, shown in Figure 30, is provided to measure mass flow during a LOCE. The drag measurement device consists of a variable reluctance transformer (VRT) force transducer to which a diamond-shaped drag arm is attached. This drag arm protrudes into and across the flow path provided by the guide tube and gives a momentum flux measurement averaged across the flow area.

5.1.2 Support Tubes. In the upper head region are also two tubes each with a 0.98-cm inside diameter intended to simulate the support columns in a full-sized PWR. In each of these tubes, a mass flow measurement is provided by the use of drag devices that have the same configuration as described in the previous paragraph for the guide tube.

5.1.3 Core Outlet. Figure 31 shows the core outlet hinged, multihole drag plate and the core outlet instrument housing. This drag device is intended to provide a typical momentum flux measurement of 10 000 kg/m·s^2 during a Semiscale LOCA.

5.1.4 Core Inlet. The core inlet drag lattice, installed in the core housing assembly before installation of the assembly in the Mod-3 vessel, is shown in Figure 32. Shown in front of the drag lattice is the lower core grid spacer. Typical upper range of the drag device is 13 000 kg/m·s^2.

5.1.5 Downcomer. The downcomer multihole drag plate, installed in the instrument washer with the three VRT force transducers, is shown in Figure 33. This device uses a three-point force measurement on a 90-degree separation. Use of a 90-degree separation between the force pickups, rather than a 120-degree separation, was required by the system geometry. Typical momentum flux measurement upper range is 30 000 kg/m·s^2.

5.1.6 Broken Loop. Figure 34 shows the multihole drag plate for use in the 3.40 cm ID piping of the broken loop. There are currently four of these devices installed in the broken loop, with installation planned for a fifth in the near future. Ranges vary depending on the measurement location and the break size, with the largest range being 700 000 kg/m·s^2 at Spool 45 in the cold leg. Because of the extremely high mass velocities in the broken loop these measurements are the most difficult mass measurements to make accurately in the Semiscale system.

5.1.7 Intact Loop. Three drag-density combination mass flow measurements are provided in the

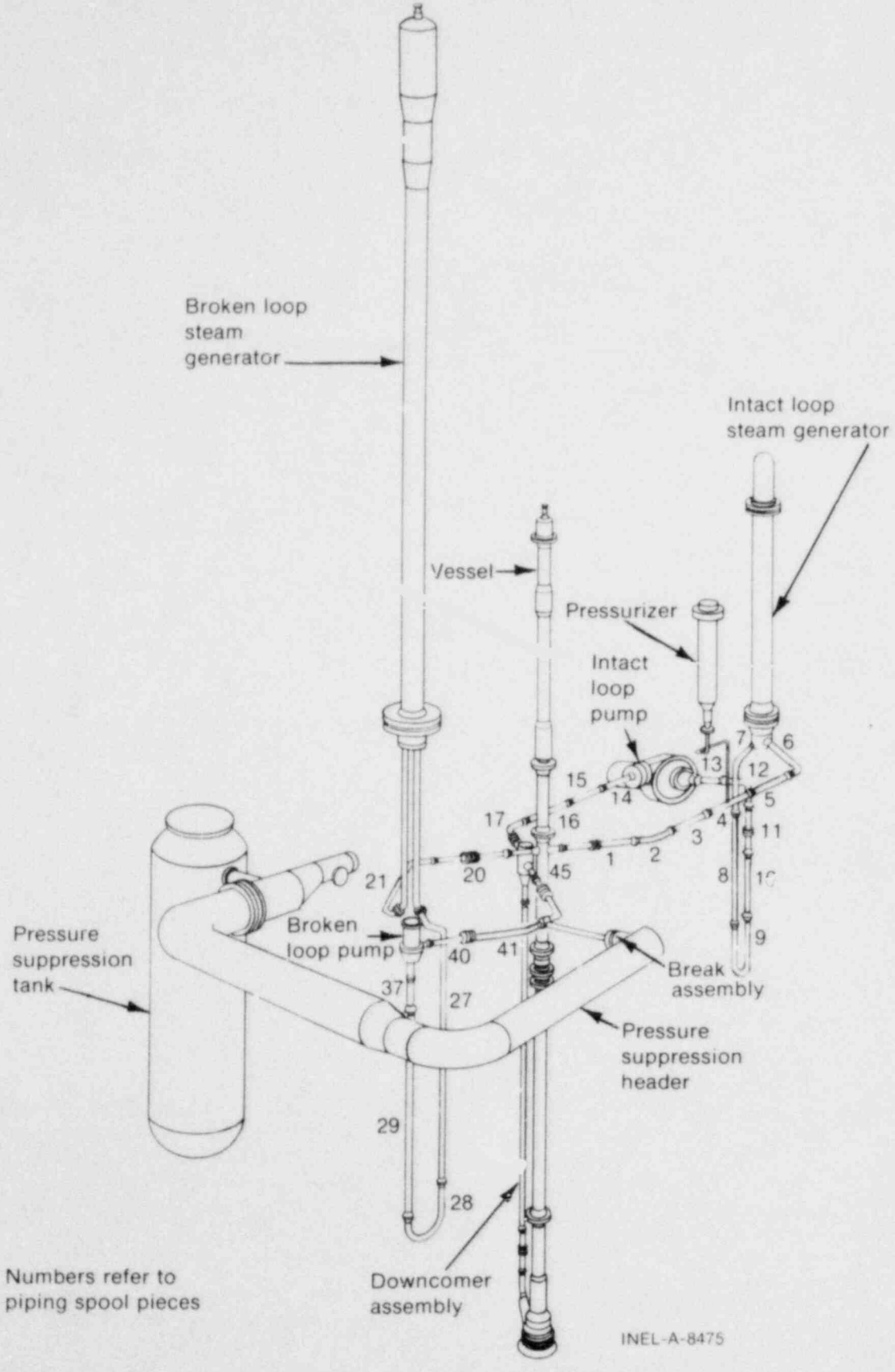

Figure 29. Semiscale Mod-3 cold leg break configuration.

Table 3. Drag Device Locations in Semiscale Mod-3 System

Location	Drag Device	Typical Momentum Flux Range[a] ($kg/m\text{-}s^2$)
Vessel		
Upper head		
Support tubes (2)	Diamond-shaped drag arm	50 000
Guide tube		10 000
Core outlet	Hinged multihole drag plate	10 000
Core inlet	Drag lattice	13 000
Downcomer	Multihole drag plate (three-point force pickup)	30 000
Broken Loop		
Spool 20		35 000
Spool 40	Hinged multihole drag plates	115 000
Spool 41		60 000 (2-1/2% break)
Spool 45		600 000
Spool 37	Drag disc	500 000
Intact Loop		
Spool 1		9 300
Spool 11	Drag disc	22 000
Spool 17		22 000

a Unless otherwise specified, ranges are given for a 200% break, simulating a double-ended pipe shear.

intact loop. Currently, all of these use drag discs such as was shown in Figure 9. Density measurements are provided by two-beam gamma densitometers.

5.2 Test Results—Test S-07-8

The Semiscale Test S-07-8 was a 200% break LOCE with the major objective being to study the effect of lower plenum ECC injection on maximum rod temperatures.

5.2.1 Core Inlet Mass Measurement. The mass flow measurement at the core inlet drag measurement location is shown in Figure 35 for the first 45 s of Test S-07-8. (The blowdown was initiated at 0 s.) The mass flow measurement shows good response time for the drag device. This measurement proves mass flow measurements can be obtained in very complex geometries.

5.2.2 Spool 45—Broken Loop Mass Measurement. The mass flow measurement at Spool Piece 45 (in the cold leg of the broken loop) is shown in Figure 36. This measurement used the hinged multihole drag plate (for 3.40-cm ID piping) in combination with a single, vertical-beam

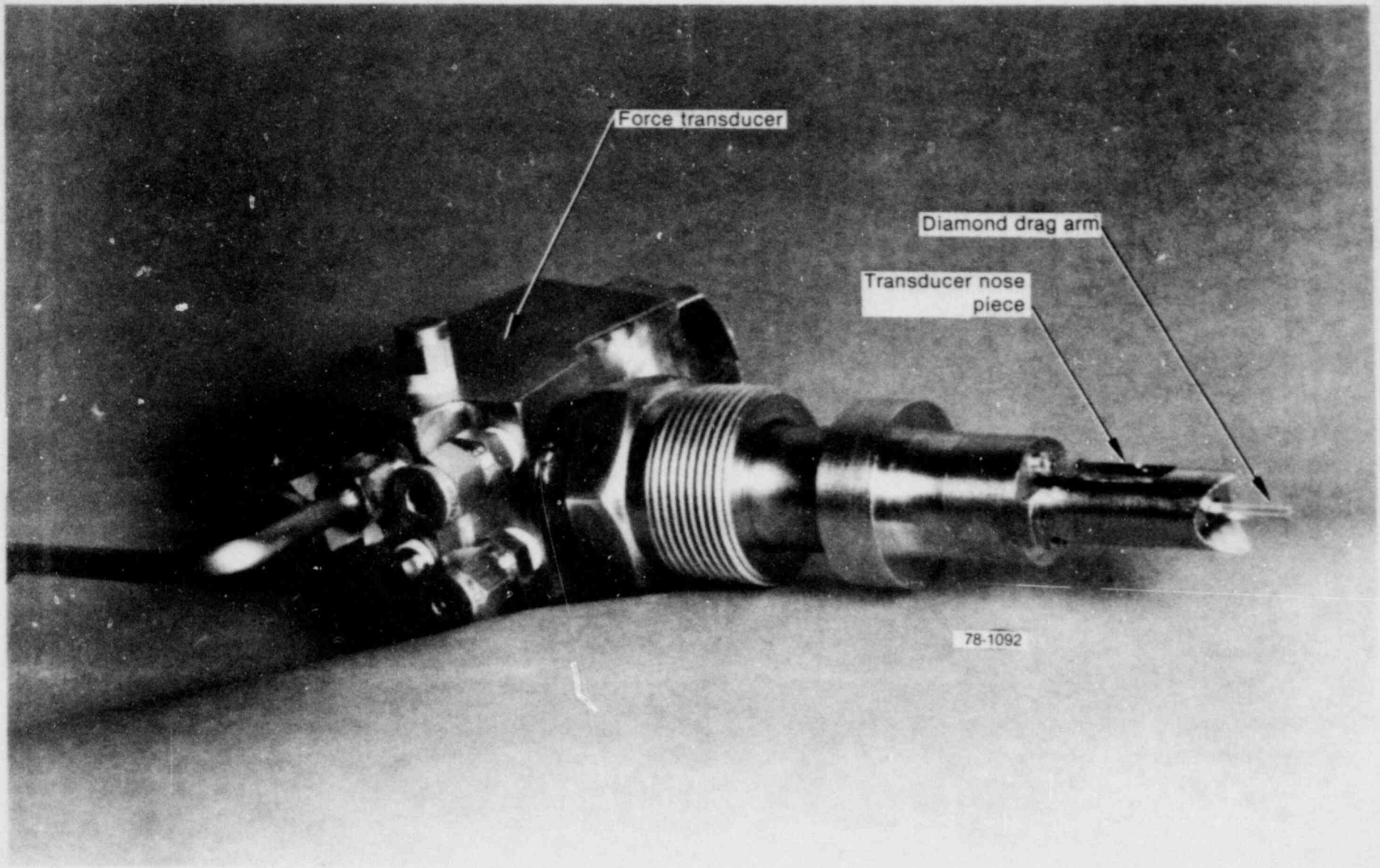

Figure 30. Semiscale VRT drag transducer with diamond-shaped drag arm for use at the guide tube measurement location.

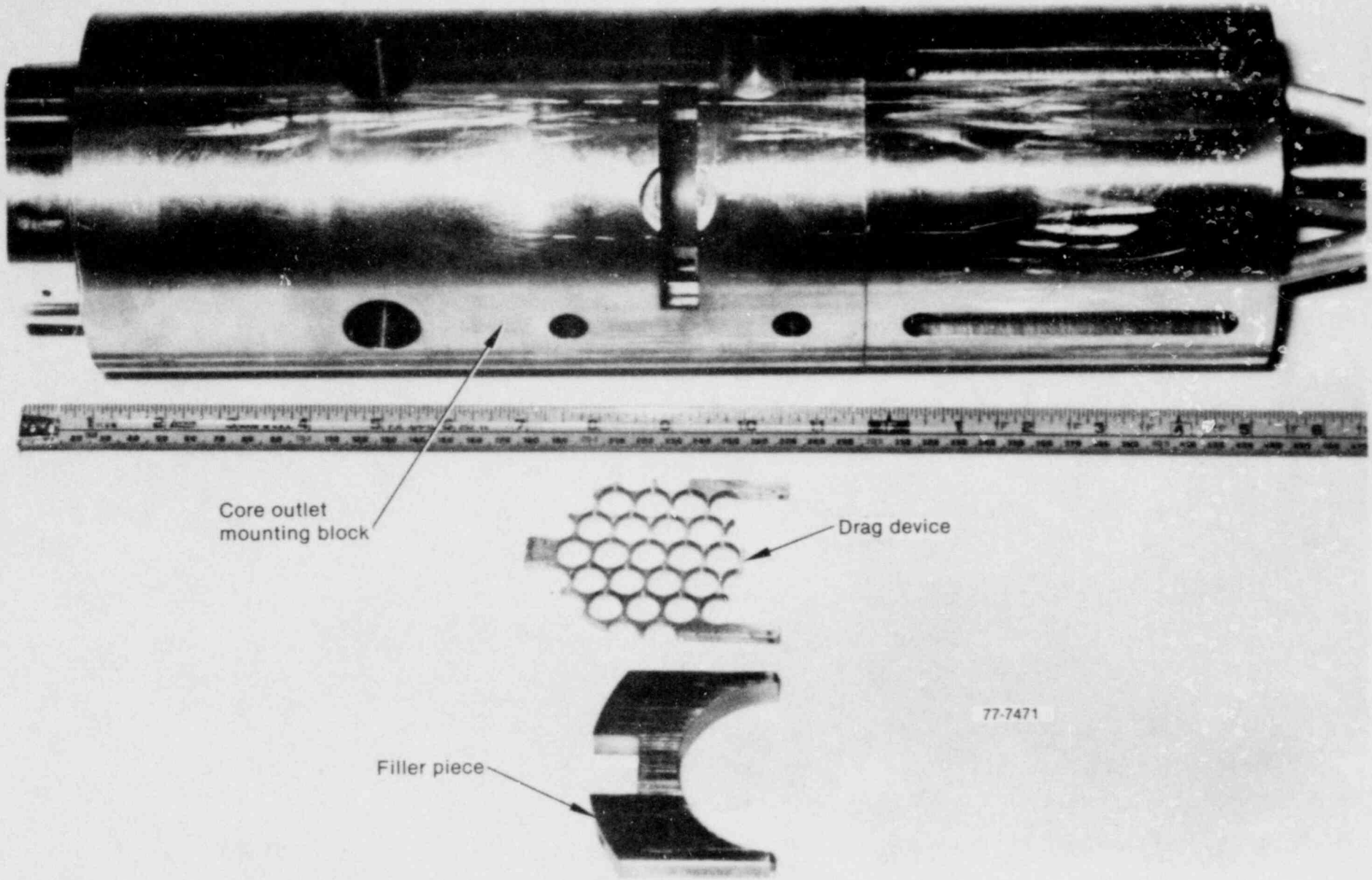

Figure 31. Hinged, multihole drag plate and instrument housing for core outlet measurement location in Semiscale Mod-3.

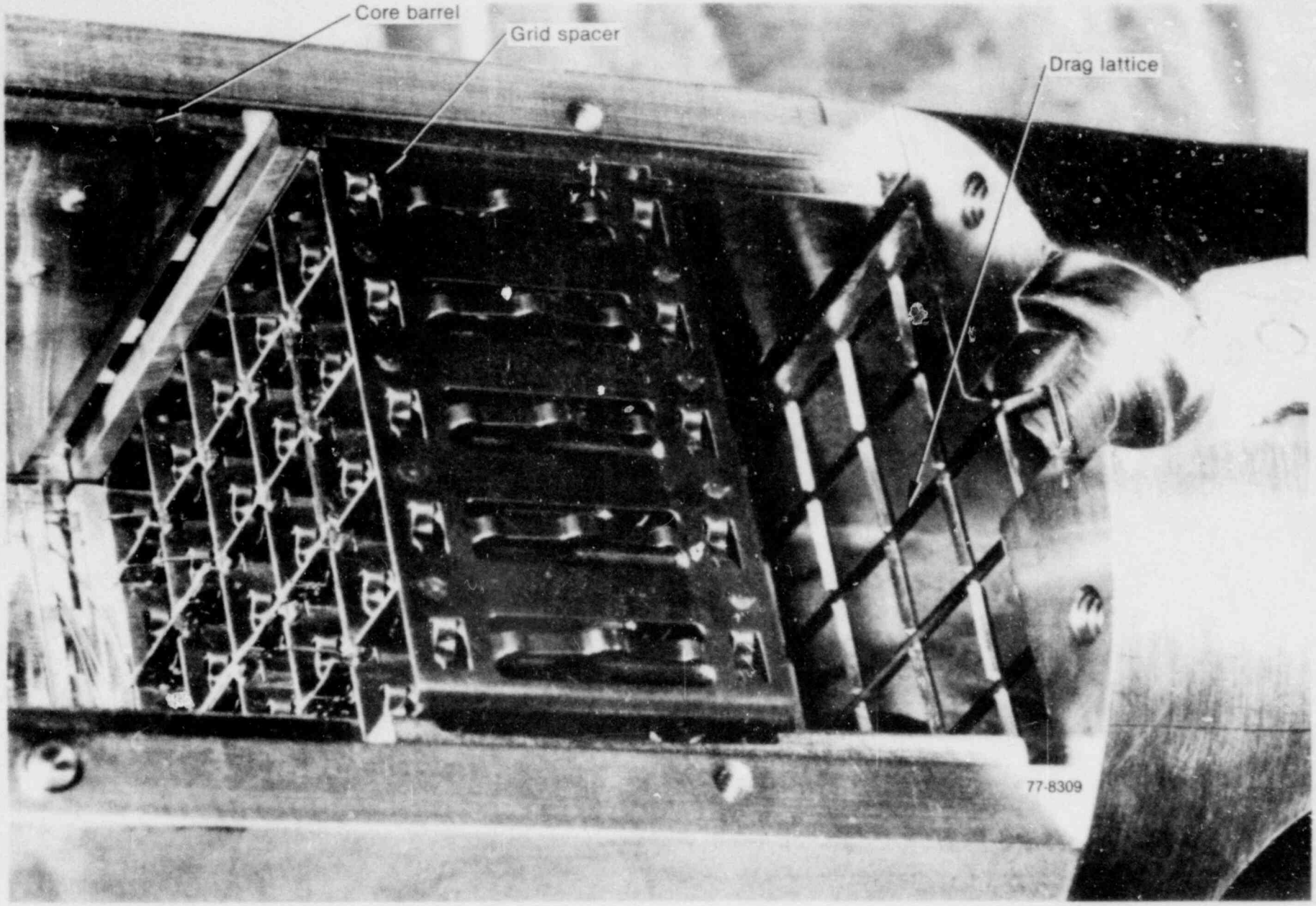

Figure 32. Core inlet drag lattice installed in core housing assembly, core grid spacer Number 1 is in front of the drag lattice.

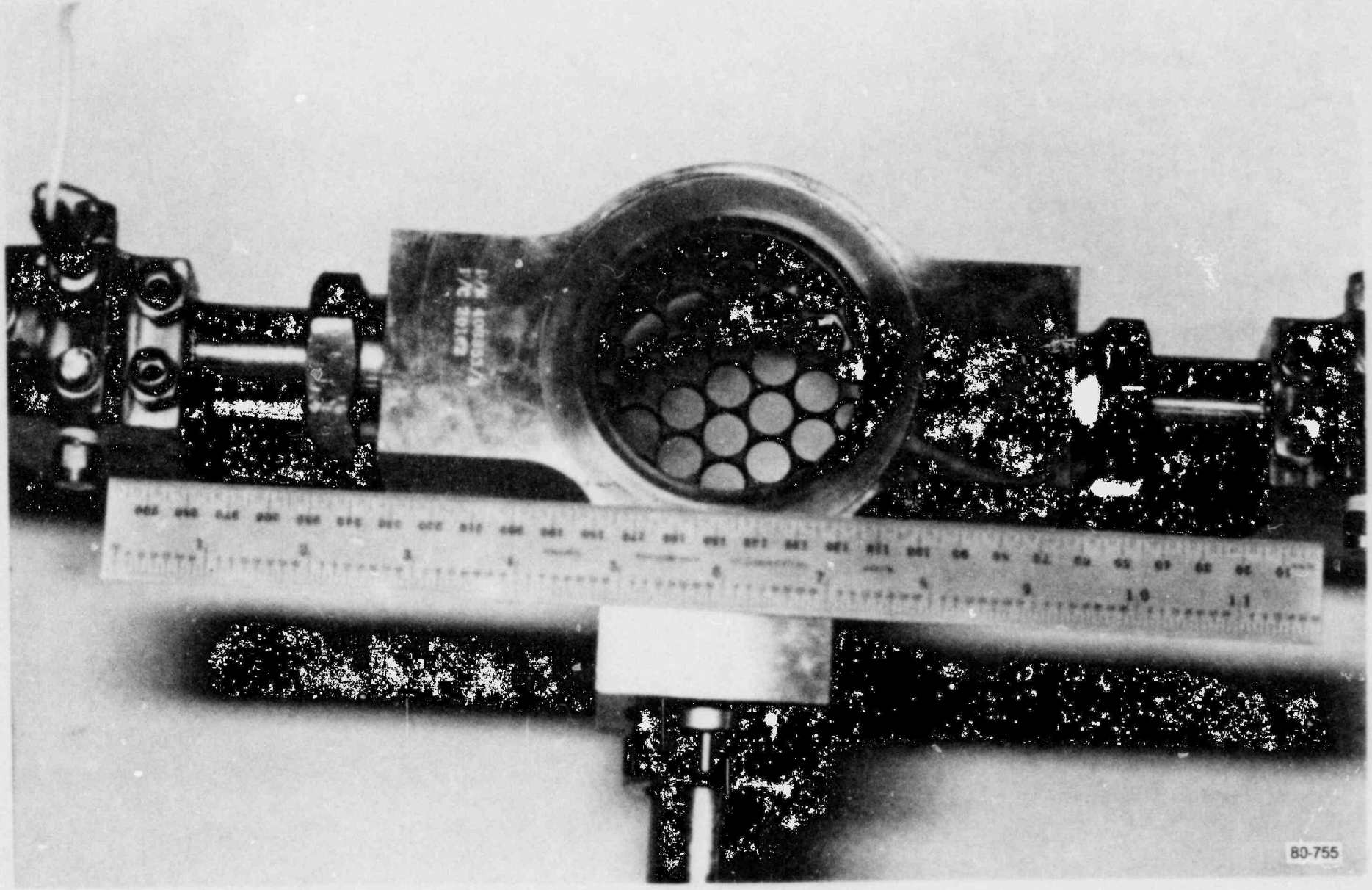

Figure 33. Multihole drag plate installed in instrument washer with three Semiscale VRT drag transducers before installation in the downcomer of Semiscale Mod-3.

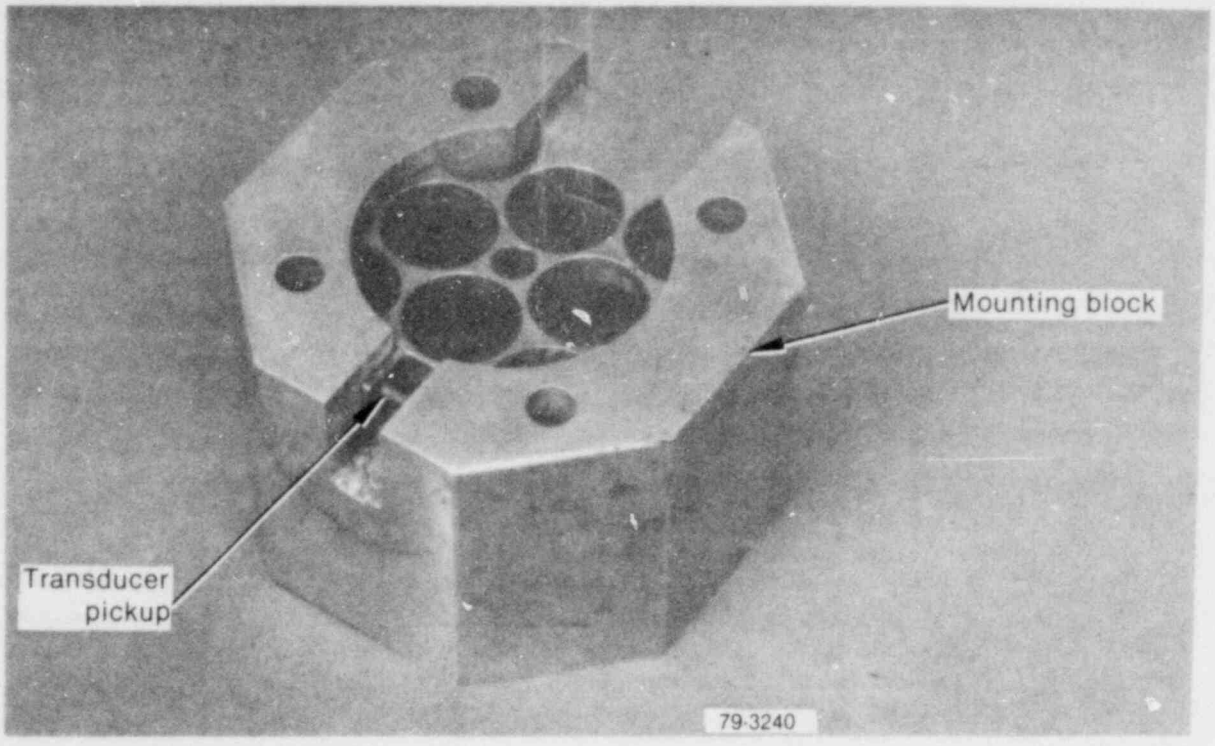

Figure 34. Hinged, multihole drag plate, shown mounted in instrument washer insert, for use in Semiscale broken loop piping (3.40 cm ID).

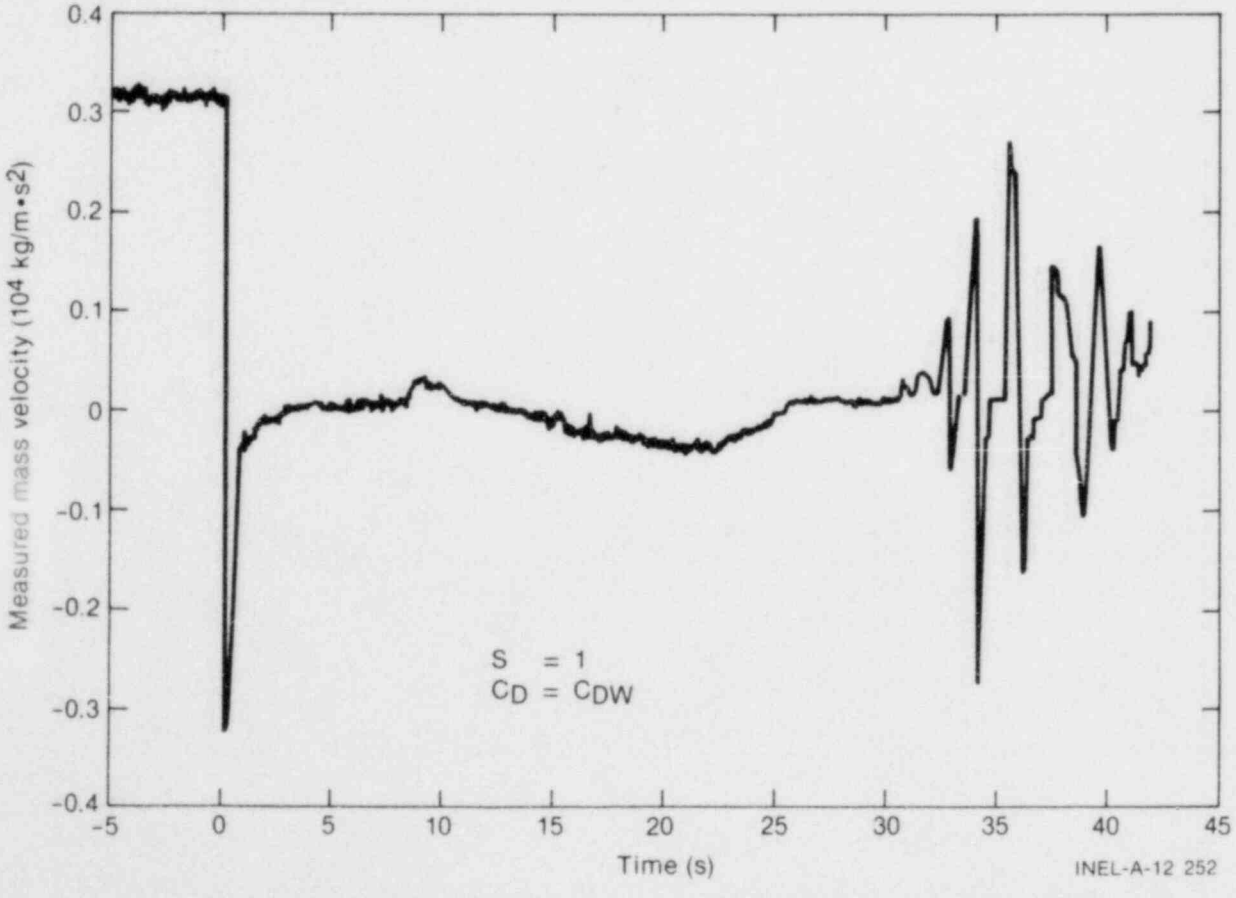

Figure 35. Mass flow measurement at core inlet measurement location of Semiscale Mod-3 vessel for Test S-07-8.

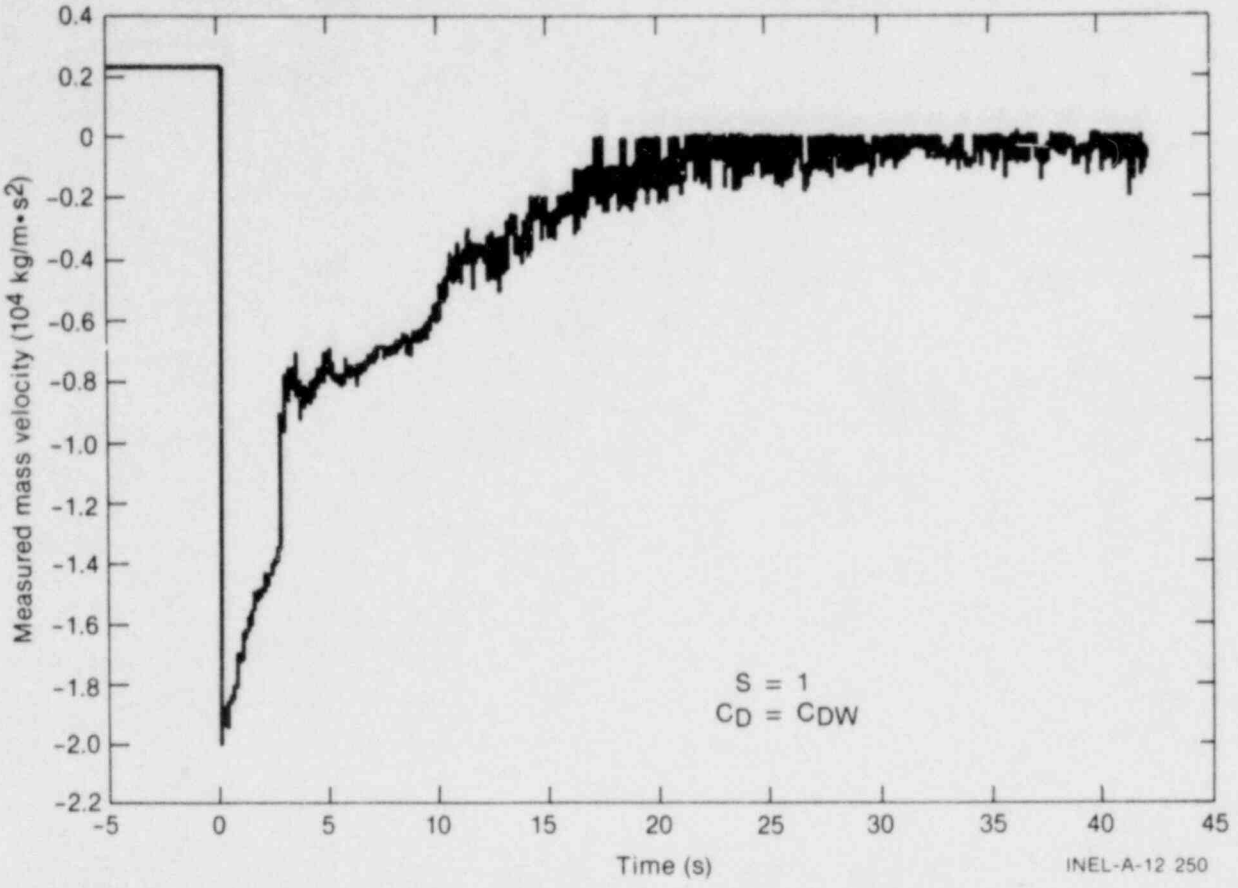

Figure 36. Mass flow measurement at Spool Piece 45 in the broken loop of the Semiscale system using hinged, multihole drag plate in combination with the vertical beam gamma densitometer. Slip of unity and C_D = constant.

gamma densitometer. A constant single-phase drag coefficient and no slip between the phases were assumed.[a] The mass velocities that were measured are about 20 000 kg/m^2·s, much higher than any of the mass velocities attainable during the air-water testing. This location experiences the largest mass velocities of any measurement location in the Semiscale system. As such, two-phase effects on a drag measurement will have the greatest effects at this location. In an attempt to investigate these effects and to allow for a reduction in the drag device range (so that the drag device would be used predominately for the two-phase measurements rather than being ranged for the initial subcooled spikes), a two-tube Pitot tube rake[b] was installed immediately downstream of the drag device facing towards the vessel. Figure 37 shows a Pitot tube rake before installation. Results from a power law fit for the velocity profile to the two Pitot tubes, in combination with a vertical beam gamma densitometer, are shown in Figure 38. Results from the drag plate and the Pitot tubes are in very close agreement, although during the initial portion of blowdown, the Pitot tubes measured a 7% higher mass velocity than the drag plate. This higher mass velocity is probably due to the faster response time of the differential pressure transducers used in conjunction with the Pitot tubes. In this measurement, the individual Pitot tubes are measuring the dynamic pressure of the fluid which is equal to the local momentum flux of the fluid at the Pitot tube.[c]

---

a. An iterative calculational routine is not currently being used to account for slip and the variable drag coefficient due to the lack of an adequate drag coefficient correlation for flow regimes other than annular mist.

b. A Pitot tube is a traditional instrument for measuring the velocity of a fluid flow. It is used to measure the dynamic pressure of the fluid and thus is sensitive to momentum flux. The Pitot tube rake was installed downstream of the drag plate with the Pitot tubes facing away from the flow direction during normal flow, which results in the Pitot tubes being upstream of the device during the reverse flow following blowdown and explains why the Pitot tube measurement was negative before t = 0.

c. References 3 and 10 provide a more complete description of mass flow measurements in two-phase flows using Pitot tubes.

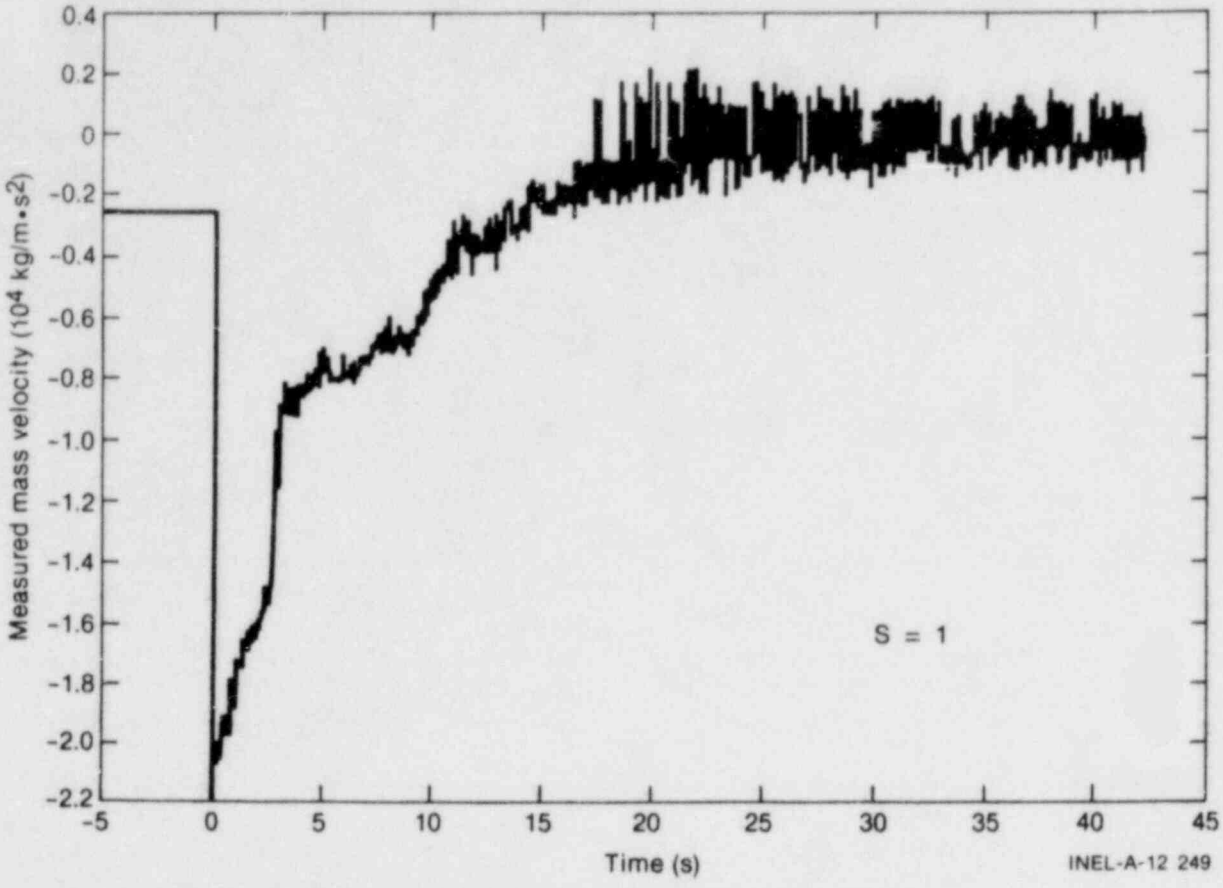

Figure 37. Pitot tube rake before installation in Spool Piece 45 of the broken loop in the Semiscale system.

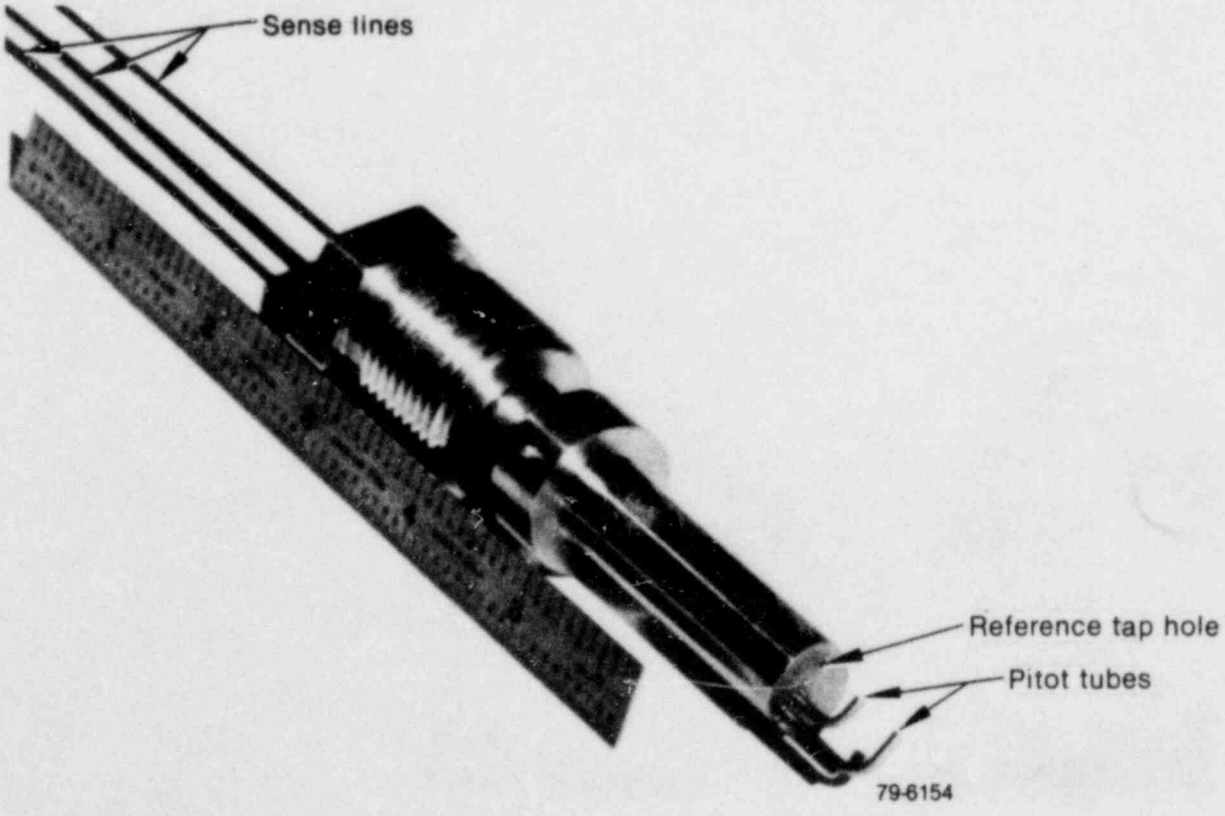

Figure 38. Mass flow measurement at Spool Piece 45 in the broken loop of the Semiscale system using a Pitot tube in combination with the single vertical beam gamma densitometer.

6. FUTURE APPLICATIONS—LOFT

LOFT provides test data to assess and improve analytical methods used to predict PWR behavior under LOCA conditions; to evaluate the performance of PWR engineered safety features, particularly the ECCS; and to assess the safety margins inherent in the performance of the engineered safety features.

The LOFT Integral Test Facility was designed to simulate the major components and system responses of a PWR involved in a LOCA and includes a containment structure, support buildings, and a test assembly that holds the 55-MW(t) pressurized water reactor that is a scaled facility approximately 1/60 the size of a modern PWR. Primary loop piping is fabricated from 14-in. Schedule 160 pipe with an inner diameter of 28.4 cm. Figure 39 is an isometric of the LOFT system within the containment building. Since the primary piping in LOFT is large-diameter pipe, the possible applications of full-flow drag devices is rather limited. The only anticipated future application of a full-flow drag device within the LOFT system is to measure the mass flow rate of the mass exiting the system for a very small break similar to the break that occurred at the Three Mile Island plant in March 1979. For this measurement, a full-flow drag device, very similar to the LOFT prototype shown in Figure 14, is to be installed on the cold leg between the break orifice and the QOBV leading to the pressure suppression vessel. Figure 40 shows the configuration of the drag device-densitometer measurement. Another future application of full-flow drag devices within LOFT is for the break flow measurement for a very small break at the pressurizer.

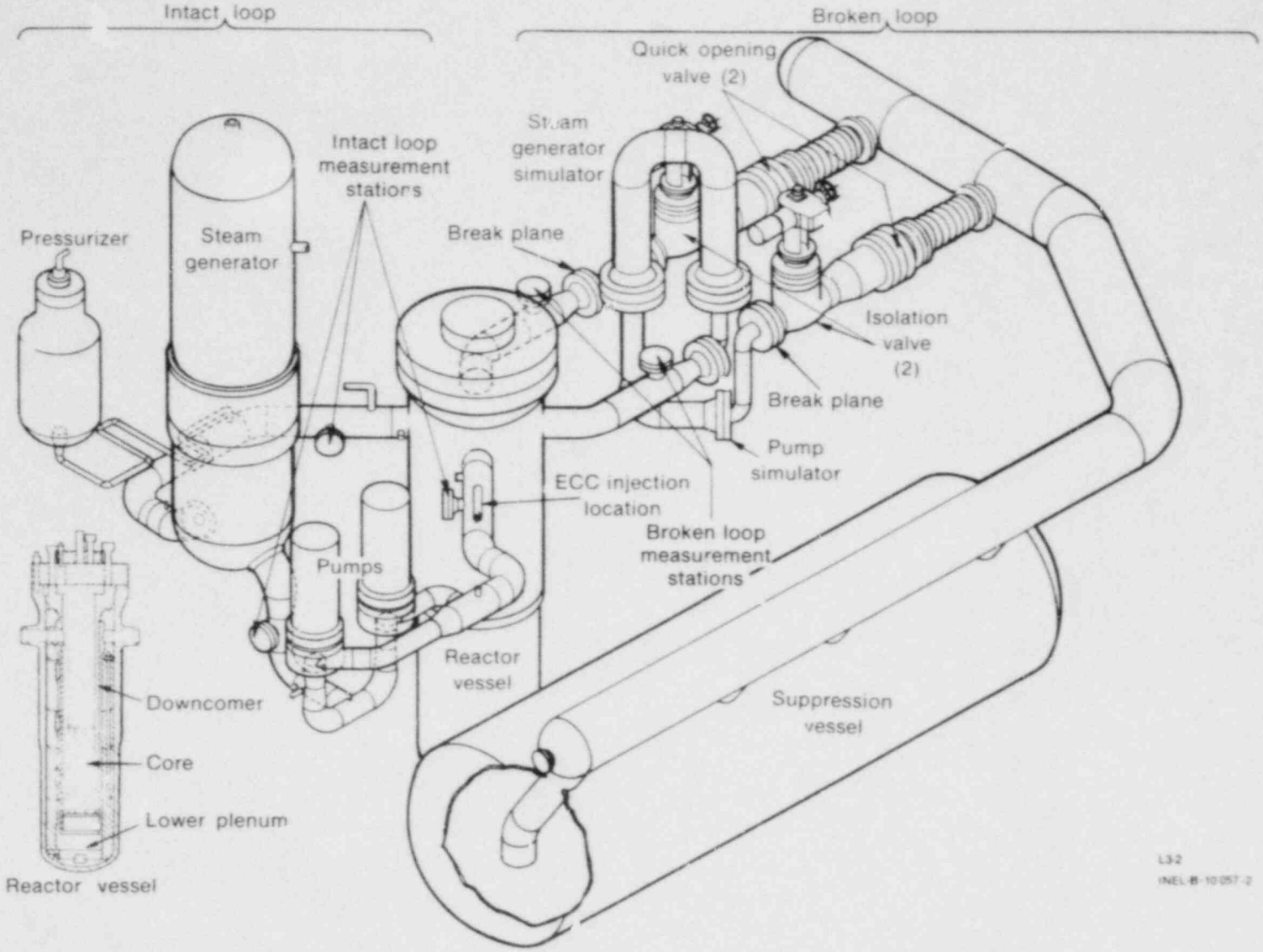

Figure 39. Isometric view of the LOFT test assembly.

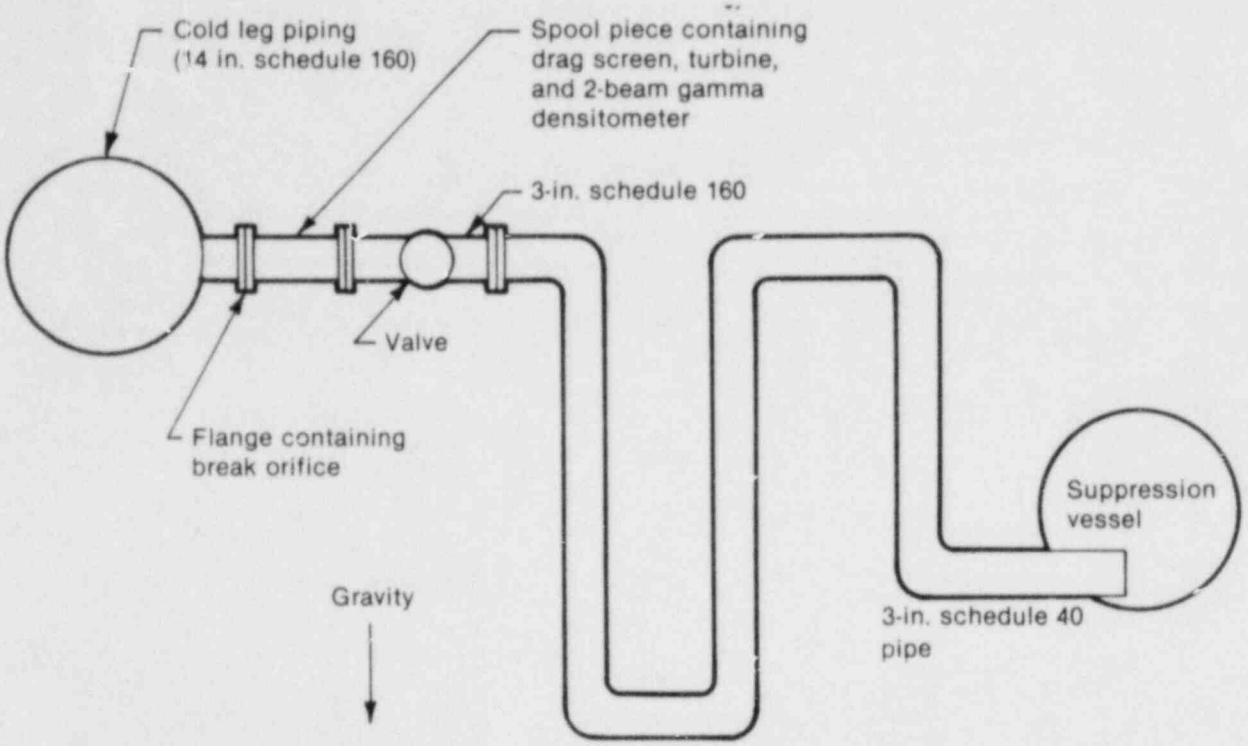

Figure 40. LOFT instrument locations—schematic for break mass flow measurement on Tests L3-5 and L3-6 shown cross-sectionally.

7. CONCLUSIONS

Steady-state, air-water testing of full-flow drag devices has proven that accurate (to within about 5%) mass flow measurements can be obtained in two-phase flows using a full-flow drag device in combination with a densitometer by the use of fairly crude analytical models. However, the accuracy is considerably less than that obtainable in single-phase flows. To improve the mass flow measurement accuracy requires the use of more sophisticated models to account for the compressibility effects on the drag coefficient and the effect of slip between the phases. A correlation for the drag coefficient on the basis of the parameter αG has been presented which greatly reduces the measurement errors in annular mist flow regimes. Results have been presented using this correlation for the drag coefficient, in combination with a slip correlation on the basis of the Hughmark-Pressburg coefficient, which reduced the measurement error from 4.8% when using a slip of unity and a constant drag coefficient, to 0.5% when using both correlations.

In circumstances in which the momentum flux profile is not skewed due to a flow disturbance upstream of the drag measurement, a hinged drag device provides as accurate a measurement as a three-point force measurement technique. However, caution must be exercised in that the measurement error may be considerable if a hinged drag device is used downstream of a flow disturbance, such as an elbow.

Design considerations for a full-flow drag device used to measure mass flow in a two-phase flow should include designing for a minimum flow blockage caused by the drag body, while still sampling over the entire flow (full flow). The amount of this flow blockage depends on the particular use and piping size; however, a flow blockage of 15 to 20% seems to be optimum and usually attainable. In addition, the type of drag device (screen, multihole, lattice) should be chosen to minimize the Reynolds Number dependency of the single-phase drag coefficient.

One of the areas in which considerable work is still to be done is flow modeling, both for description of the flow and description of the effects on a drag body inserted into the flow (drag coefficients).

8. REFERENCES

1. J. L. Anderson and J. R. Fincke, "Mass Flow Measurements in Air-Water Mixtures Using Drag Devices and Gamma Densitometer," *Proceedings of Twenty-Fourth ISA International Instrumentation Symposium, Albuquerque, New Mexico, May 1978.*

2. J. L. Anderson, "Air-Water Testing of a Full-Flow Drag Screen for Mass Flow Measurements," *Quarterly Technical Progress Report on Water Reactor Safety Programs sponsored by the Nuclear Regulatory Commission's Division of Reactor Safety Research*, TREE-NUREG-1213, April 1978.

3. J. R. Fincke, *Development of the LOFT Prototype Drag Screen—Air-Water Testing*, TREE-NUREG-1195, May 1978.

4. J. R. Fincke, *Development of the LOFT Prototype Drag Screen—Transient Steam-Water Testing*, NUREG/CR-0270, TREE 1241, July 1978.

5. G. D. Lassahn, *LOFT Three-Beam Densitometer Interpretation*, TREE-NUREG-1111, October 1977.

6. G. T. Lilly et al., *1/14-Scale Steam/Water Mixing Report*, WCAP-8307, September 1974.

7. G. A. Hughmark and B. S. Pressburg, "Holdup and Pressure Drop with Gas-Liquid Flow in a Vertical Pipe," *American Institute of Chemical Engineers Journal*, December 1961, pp. 677-682.

8. J. M. Mandhane et al., "A Flow Pattern Map for Gas-Liquid Flow in Horizontal Pipes," *International Journal Multiphase Flow, 1*, 1974, pp. 537-553.

9. M. L. Patton, *Semiscale Mod-3 Test Program and System Description*, NUREG/CR-0239, TREE-1212, July 1978.

10. J. R. Fincke and V. A. Deason, *The Measurement of Phase Velocities in Mist Flows Using Stagnation Probes*, NUREG/CR-0648, TREE-1350, March 1979.